Interpretation of long-term measurements of radiatively active trace gases and ozone depleting substances

DECC contract number: GA0201

Quarterly Report (November 2012 - January 2013)

Date: 31st Jan 2013

Authors:
Alistair J. Manning (Met Office),
Simon O'Doherty, Aoife Grant (University of Bristol),
Dickon Young (Terra Modus),
Richard G. Derwent (rdscientific),
Peter Simmonds (INSCON)

Contents

1 Executive Summary

1.1 Project Summary

Monitoring of atmospheric concentrations of gases is important in assessing the impact of international policies related to the atmospheric environment. The effects of control measures on chlorofluorocarbons (CFCs), halons and HCFCs introduced under the 'Montreal Protocol of Substances that Deplete the Ozone Layer' are now being observed. Continued monitoring is required to assess the overall success of the Protocol and the implication for atmospheric levels of replacement compounds such as HFCs. Similar analysis of gases regulated by the Kyoto Protocol on greenhouse gases will likewise assist policy makers.

Since 1987, high-frequency, real time measurements of the principal halocarbons and radiatively active trace gases have been made as part of the Global Atmospheric Gases Experiment (GAGE) and Advanced Global Atmospheric Gases Experiment (AGAGE) at Mace Head, County Galway, Ireland. For much of the time, the measurement station, which is situated on the Atlantic coast, monitors clean westerly air that has travelled across the North Atlantic Ocean. However, when the winds are easterly, Mace Head receives substantial regional scale pollution in air that has travelled from the industrial regions of Europe. The site is therefore uniquely situated to record trace gas concentrations associated with both the mid-latitude Northern Hemisphere background levels and with the more polluted air arising from Europe.

The observation network in the UK has been expanded to include three additional stations; Angus Tower near Dundee, Tacolneston near Norwich and Ridge Hill near Hereford. Ridge Hill became operational in February 2012, Tacolneston began operating in July 2012 and Angus Tower has been making measurements since late 2005.

The Met Office's Lagrangian atmospheric dispersion model, NAME (**N**umerical **A**tmospheric dispersion **M**odelling **E**nvironment), has been run for each 2-hour period of each year from 1989 so as to understand the recent history of the air arriving at Mace Head at the time of each observation. By identifying when the air is unpolluted at Mace Head, i.e. when the air has travelled across the Atlantic and the air concentration reflects the mid-latitude Northern Hemisphere baseline value, the data collected have been used to estimate baseline concentrations, trends and seasonal cycles of a wide range of ozone-depleting and greenhouse gases for the period 1989-2012 inclusive.

By removing the underlying baseline trends from the observations and by modelling the recent history of the air on a regional scale, estimates of UK, Irish and North West European (UK, Ireland, France, Germany, Denmark, the Netherlands, Belgium, Luxembourg) emissions and their geographical distributions have been made using InTEM (Inversion Technique for Emission Modelling). The estimates are presented as yearly averages and are compared to the UNFCCC inventory.

The atmospheric measurements and emission estimates of greenhouse gases provide an important cross-check for the emissions inventories submitted to the United Nations Framework Convention on Climate Change (UNFCCC). This verification work is consistent with good practice guidance issued by the Intergovernmental Panel on Climate Change (IPCC).

2 Overview of Progress

The Mace Head observation station continues to operate effectively and there are no data issues to report.

Tacolneston has been operating well since installation in July 2012. Many Medusa compounds have improved in precision considerably after implementation of new methodology.

The electron capture detector at Ridge Hill is being replaced due to damage. Its damage has resulted in 2 months of lost data.

The operation of Tall Tower Angus has transferred to the University of Bristol.

Atmospheric baseline concentrations for each gas reported at Mace Head have been estimated through to the end of December 2012 and the website updated.

Project web site (www.metoffice.gov.uk/atmospheric-trends) now linked to DECC and University of Bristol web sites.

InTEM (INversion Technique for Emission Modelling) has been improved. The main focus of the improvement has been in assessing the baseline growth rate of each gas. Two growth rate methods are now reported on the graph to demonstrate the potential uncertainty in this important quantity.

3 Operational sites and observed species

Sites -> Species	Mace Head MHD	Tacolneston TAC	Ridge Hill RGL	Angus TTA
CO_2	Picarro 2301*(1)*	Picarro 2301*(1)*	Picarro 2301*(1)*	LiCor 7000*(1)*
CH_4	Picarro 2301(1), GC-FID*(40)*	Picarro 2301*(1)*	Picarro 2301*(1)*	GC-FID*(40)*
N_2O	GC-ECD*(40)*	GC-ECD*(20)*	GC-ECD*(20)*	GC-ECD*(40)*
SF_6	Medusa*(120)*	GC-ECD*(20)*, Medusa*(120)*	GC-ECD*(20)*	GC-ECD*(40)*
H_2	GC-RGA*(40)*	GC-RGA*(20)*	-	-
CO	GC-RGA*(40)*	GC-RGA*(20)*	-	-
CF_4	Medusa*(120)*	Medusa*(120)*	-	-
C_2F_6	Medusa*(120)*	Medusa*(120)*	-	-
C_3F_8	Medusa*(120)*	Medusa*(120)*	-	-
c-C_4F_8	Medusa*(120)*	-	-	-
HFC-23	Medusa*(120)*	Medusa*(120)*	-	-
HFC-32	Medusa*(120)*	Medusa*(120)*	-	-
HFC-134a	Medusa*(120)*	Medusa*(120)*	-	-
HFC-152a	Medusa*(120)*	Medusa*(120)*	-	-
HFC-125	Medusa*(120)*	Medusa*(120)*	-	-
HFC-143a	Medusa*(120)*	Medusa*(120)*	-	-
HFC-227ea	Medusa*(120)*	Medusa*(120)*	-	-
HFC-236fa	Medusa*(120)*	Medusa*(120)*	-	-
HFC-43-10mee	Medusa*(120)*	-	-	-
HFC-365mfc	Medusa*(120)*	Medusa*(120)*	-	-
HFC-245fa	Medusa*(120)*	Medusa*(120)*	-	-
HCFC-22	Medusa*(120)*	Medusa*(120)*	-	-
HCFC-141b	Medusa*(120)*	Medusa*(120)*	-	-
HCFC-142b	Medusa*(120)*	Medusa*(120)*	-	-
HCFC-124	Medusa*(120)*	Medusa*(120)*	-	-
HCFC-123	-	Medusa*(120)*	-	-
CFC-11	Medusa*(120)*	Medusa*(120)*	-	-
CFC-12	Medusa*(120)*	Medusa*(120)*	-	-
CFC-13	Medusa*(120)*	Medusa*(120)*	-	-
CFC-113	Medusa*(120)*	Medusa*(120)*	-	-
CFC-114	Medusa*(120*	Medusa*(120)*	-	-
CFC-115	Medusa*(120)*	Medusa*(120)*	-	-
H-1211	Medusa*(120)*	Medusa*(120)*	-	-
H-1301	Medusa*(120)*	Medusa*(120)*	-	-
H-2402	Medusa*(120)*	Medusa*(120)*	-	-
CH_3Cl	Medusa*(120)*	Medusa*(120)*	-	-
CH_3Br	Medusa*(120)*	Medusa*(120)*	-	-
CH_3I	Medusa*(120)*	Medusa*(120)*	-	-
CH_2Cl_2	Medusa*(120)*	Medusa*(120)*	-	-
CH_2Br_2	Medusa*(120)*	Medusa*(120)*	-	-
$CHCl_3$	Medusa*(120)*	Medusa*(120)*	-	-
$CHBr_3$	Medusa*(120)*	Medusa*(120)*	-	-
CCl_4	Medusa*(120)*	Medusa*(120)*	-	-
CH_3CCl_3	Medusa*(120)*	Medusa*(120)*	-	-
$CHCl=CCl_2$	Medusa*(120)*	Medusa*(120)*	-	-
$CCl_2=CCl_2$	Medusa*(120)*	Medusa*(120)*	-	-

Table 1: Operational sites, instrumentation and observed species. Number in brackets indicates frequency of calibrated air measurement in minutes.

4 Update on three UK sites

4.1 Angus Tower

Just prior to the UK DECC network meeting in December 2012, University of Edinburgh contacted the University of Bristol to inform them that they could no longer continue to run the Angus site. It was suggested that the University of Bristol could manage the site and run the instruments in the following months. The University of Bristol are in the process of transferring the site sharing agreement with Arqiva from the University of Edinburgh to the University of Bristol. Internet and telephone accounts will also be transferred. It is proposed that only the Picarro CRDS instrument be maintained for the final year of the DECC contract measuring CO_2 and CH_4 only. All other instruments will be mothballed until funds are made available to allow their overhaul and update to the standard of existing equipment in the DECC network, or the purchase of new equipment.

CO_2 data from Angus is currently measured by a LiCor 7000 in line with the contract. However data from the Picarro 1301 instrument which has been at the site since the beginning of the current DECC contract has been made available to the project. The Picarro 1301 provides measurements of CO_2 and CH_4. CO_2 data from this more modern instrument is thought to be more precise than the older LiCor. We are in the process of automating the transfer of this raw Picarro data to the Integrated Carbon Observation System (ICOS) server (free of charge) for processing and data validation.

The GC-ECD at Angus, which measures N_2O and SF_6 was previously operating with problems (and a very high background signal). The ECD detector was replaced in December 2011. The new detector gave a low background and data quality improved for N_2O and SF_6. Very recent N_2O data appears to overlay well with Mace Head measurements, albeit with a constant baseline offset (Figure 1). From visual inspection SF_6 data overlays well with Mace Head data. CH_4 data overlays well with Mace Head but the magnitude of pollution events are smaller at Angus than Mace Head which is contrary to what would be expected considering the sites location. One possible reason for this could be that the sample line is contaminated with algae which may consume CH_4 (or N_2O). Another reason could be the difference in sampling heights, with Angus samples taken from 222 m up the tower being diluted compared with samples taken from 15 m above the ground at Mace Head. Yet another cause for this difference could be due to instrument calibration issues. When CH_4 data from the Picarro 1301 instrument is calibrated it will enable us to validate the CH_4 data from the gas chromatograph with flame ionisation detector. This will clarify whether pollution events are actually of a smaller magnitude or if it is an instrumental issue. CO_2 data generally overlays well with Mace Head data however there appear to be many recent depletions in CO_2 which are not seen at Mace Head. The validity of these low CO_2 measurements will also be clarified when calibrated CO_2 data from the Picarro 1301 is available.

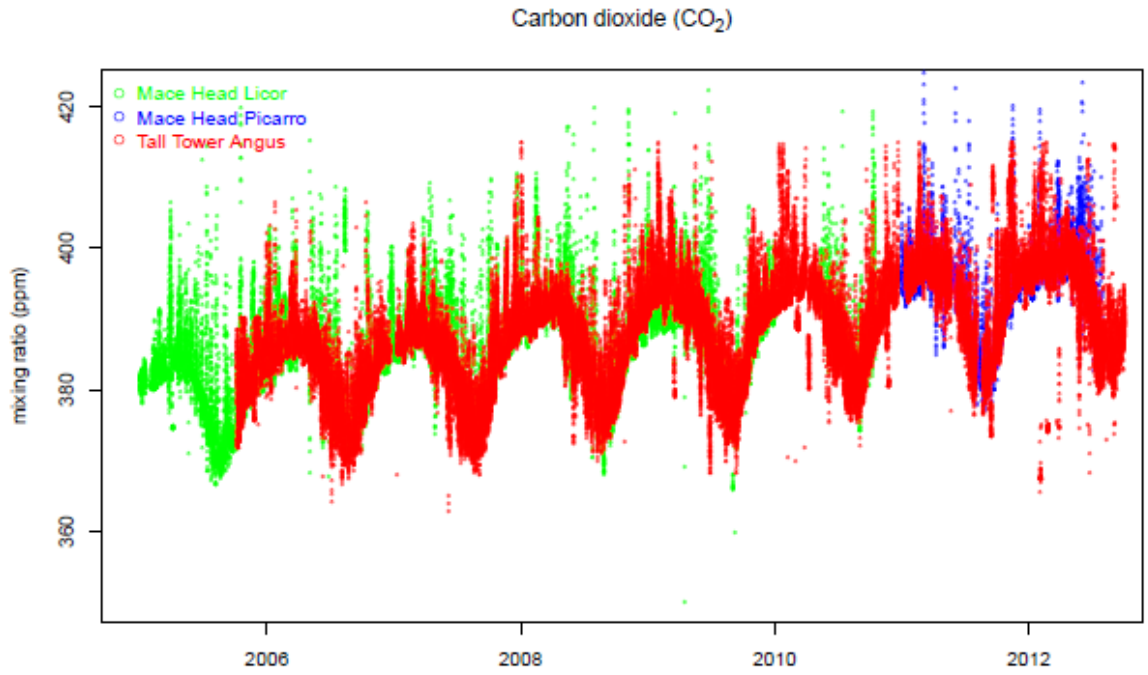

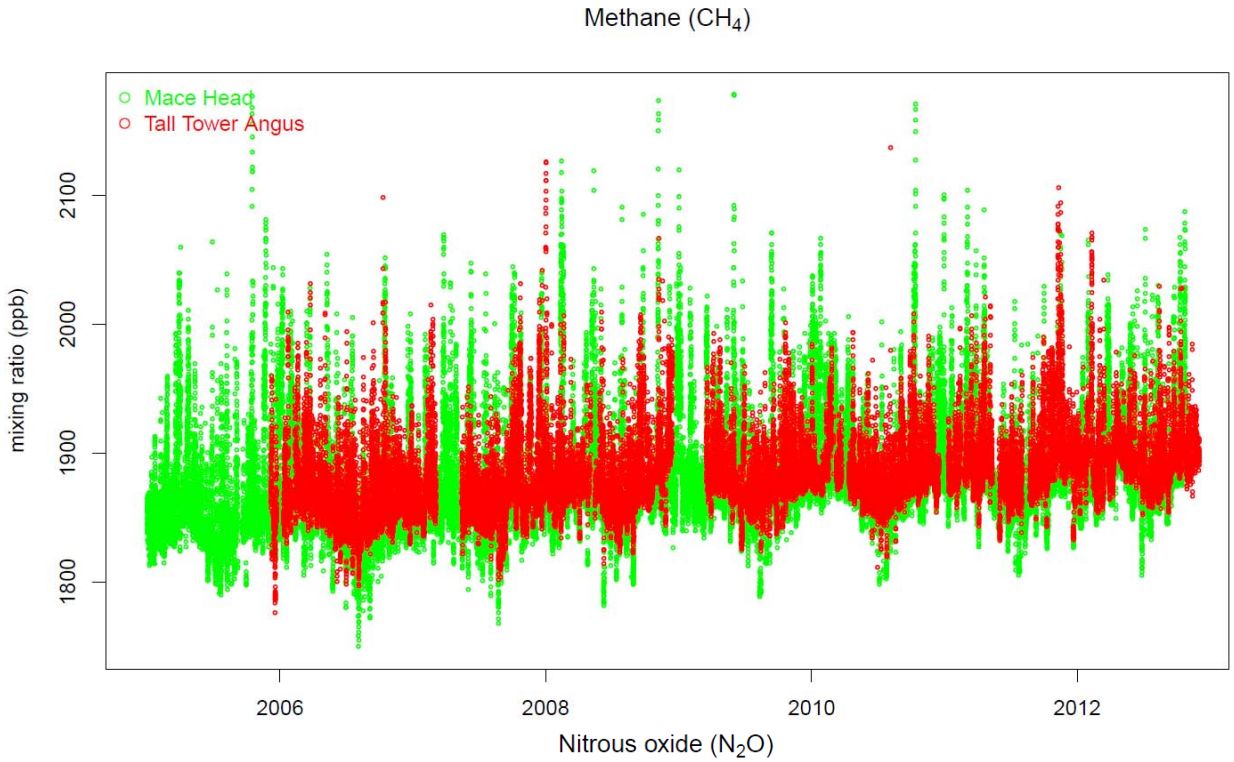

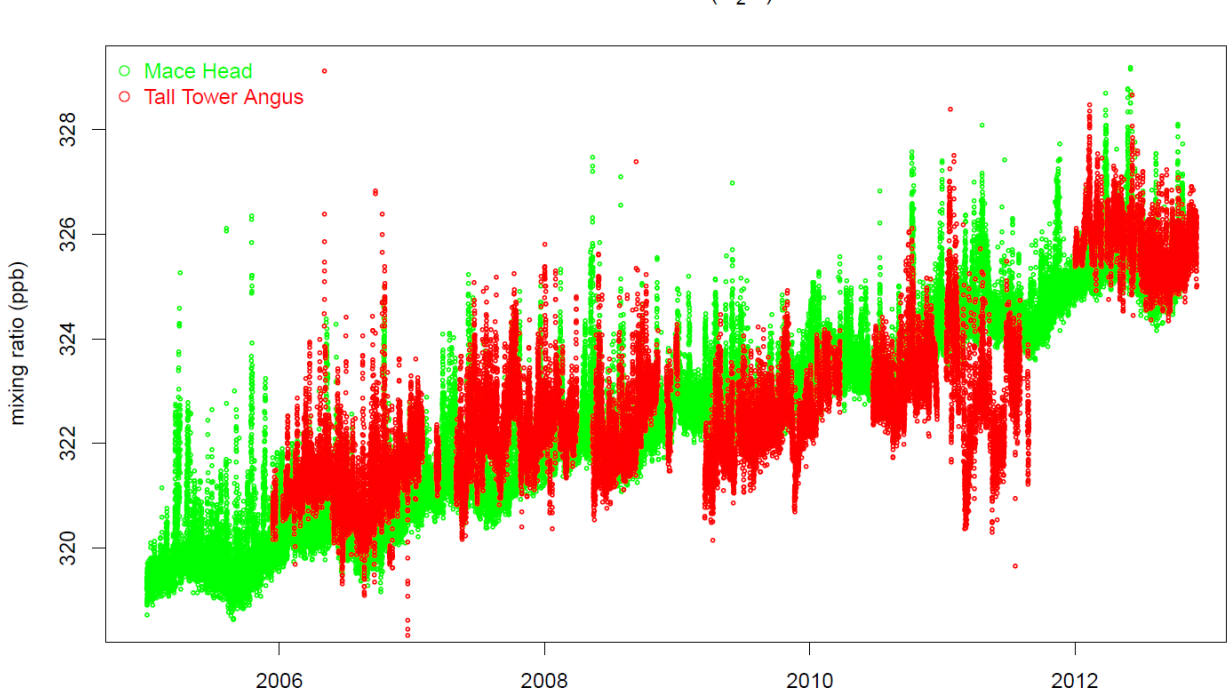

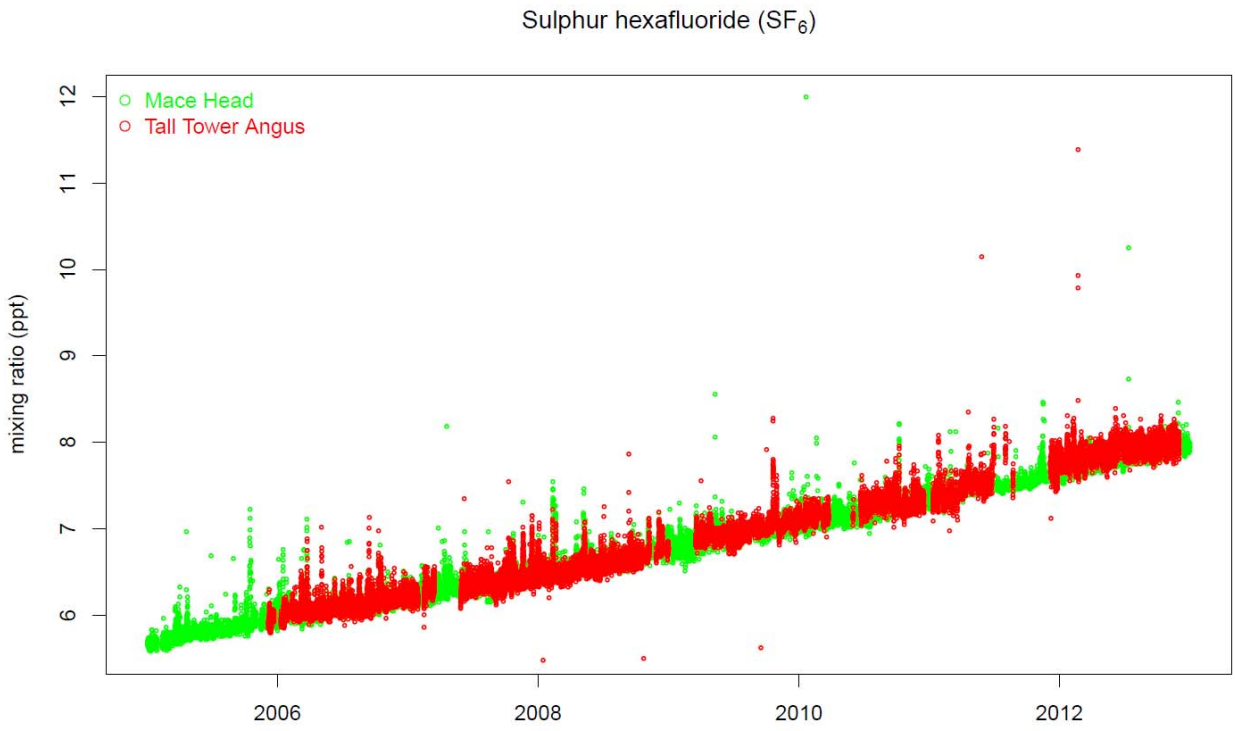

Figure 1: Angus data (red) and Mace Head data (green and blue) for CO_2, CH_4, N_2O and SF_6.

4.2 Tacolneston

The Mobile lab at Tacolneston has been operational since July 2012 and all instrumentation is operating well. An unexpected power cut occurred during on site work at Tacolneston on the 5th of December. The technician from the University of East Anglia, Stephen Humphrey was able to go onsite and restart instrumentation on the 7th of December.

In early December the Medusa mass spectrometer parameters were changed to measure the mass of ions by 'sliding' windows instead of the previous method of static windows. This resulted in a significant improvement in precision for the majority of species. Certain species, particularly CF_4, have degraded in precision because the refrigeration unit which is used to cool the traps has not been operating optimally. The cause of this problem is due to reduced amounts of refrigerant in the unit which primarily affects the most volatile species such as CF_4. A site visit is planned for the 30th of January where the coolant will be topped up and a filter on the unit changed. Other optimisations will be carried out on the instrument during this visit such as initiation of blank runs and sampling of lab air. The latter enables us to assess whether any instrument contamination may be occurring from gases inside the lab. During this site visit Stephen Humphrey, the technician who visits the site each week to service instrumentation will also undergo additional training on the instrumentation, in particular the Medusa. A comparison of the ambient record for certain Medusa species with associated standard precision are shown in Figure 2(a)-(f).

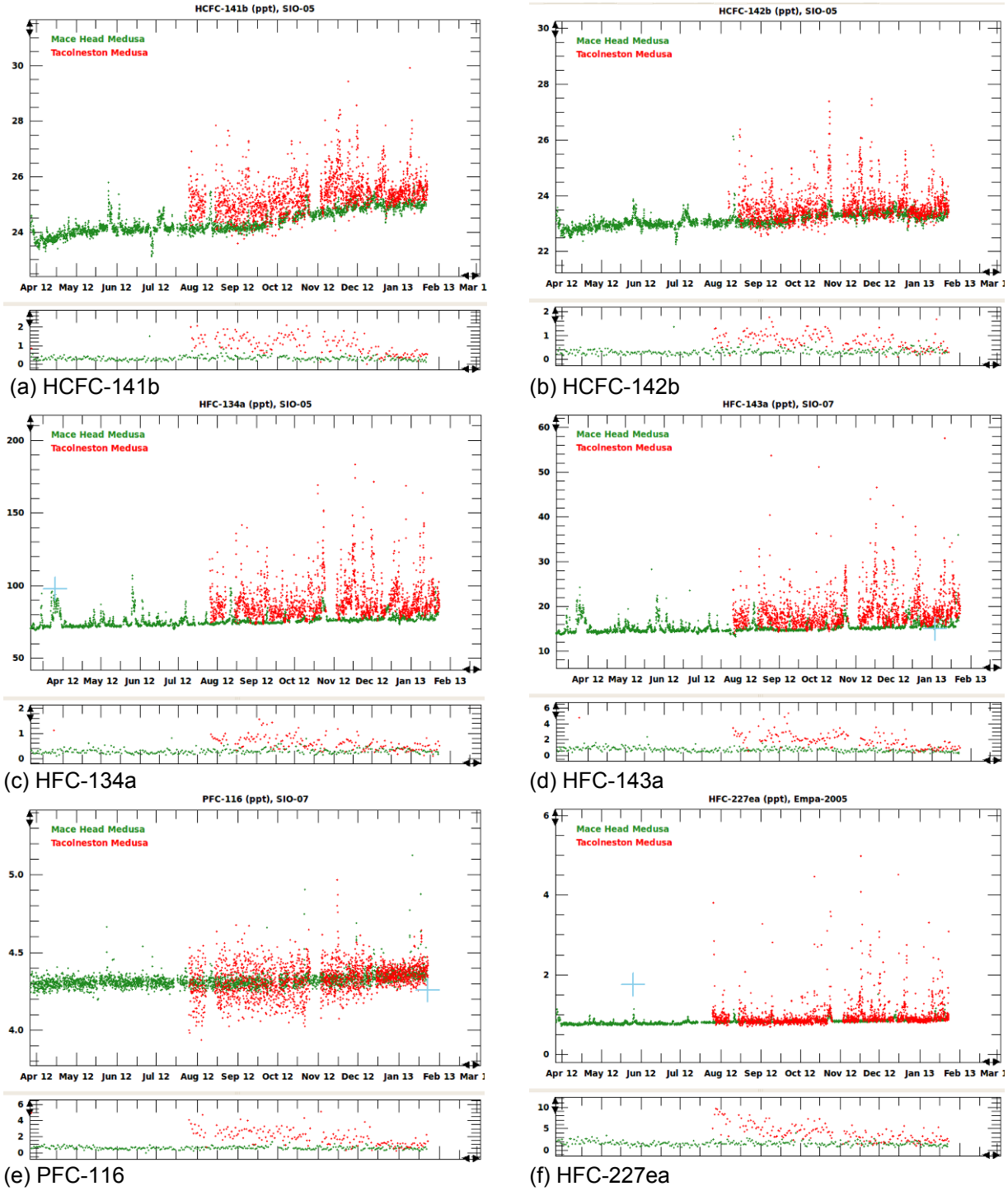

Figure 2: Comparison of selected Medusa species at Mace Head (green) and Tacolneston (red).

The MD system has been running well without any problems during the last quarter. An overlay of N_2O from Tacolneston and Mace Head is shown in Figure 3(a). A plot overlaying SF_6 data acquired by the Medusa and MD at Tacolneston demonstrate the excellent agreement obtained between the two different instruments (Figure 3).

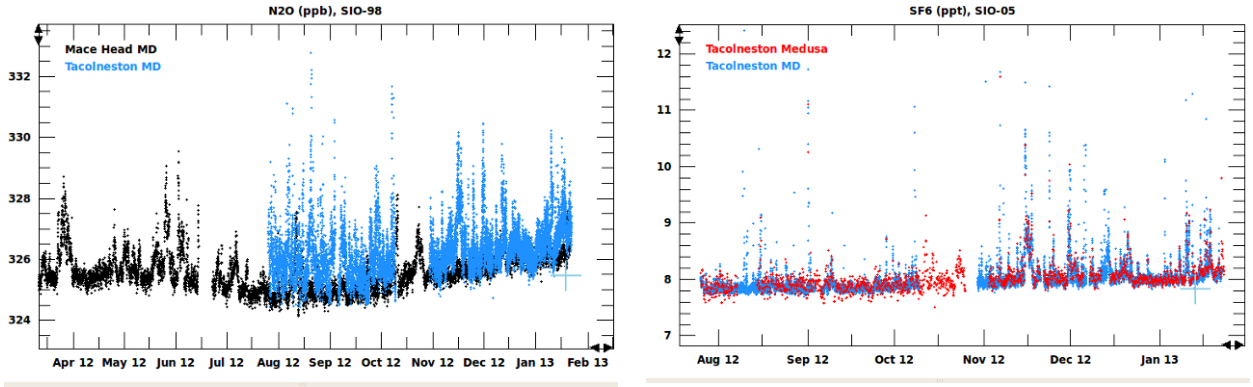

Figure 3: Right, N_2O at Mace Head (black) and Tacolneston (blue); Left, comparison of SF_6 on the GC-ECD (blue) vs Medusa (red)

The Picarro 2301 cavity ring down spectrometer (CRDS), which samples air from 100 and 50 meters has also been running well in the last quarter with no problems. The Integrated Carbon Observation System (ICOS) who currently process the raw CRDS data into calibrated data have updated their processing capabilities. On the 17th of January the new software was installed on the CRDS at Tacolneston to enable automatic data transfer to the new ICOS server.

4.3 Ridge Hill

The Picarro 2301 CRDS has been running well at Ridge Hill. The CRDS samples air from the two tower heights of 45 m and 90 m, alternating every 30 minutes. The CRDS operates by measuring CO_2 and CH_4 in an evacuated cavity at very low pressure. During the last quarter the vacuum pump used to evacuate the cavity broke twice. A more robust pump (Vacuubrand MD-1) has been purchased and will be fitted on the 4th of February to prevent any future pump failures. The automatic data transfer process was updated at Ridge Hill on the 17th of January keeping in line with the new ICOS data processing server. Data is being transferred every day to the ICOS server for processing and calibrated data returned daily to the data server held at Bristol University. A plot of data from 2012 is shown in Figure 4.

The gas chromatograph with electron capture detector (ECD), which measures N_2O, and SF_6 at Ridge Hill, ran well until the bad storms towards the end of November 2012. During heavy rain and strong winds on the 15th of November the water traps at the base of the tower overfilled and water was sucked into the instrument. The instrument was shut down and a site visit was made on the 20th of November to fix the problems which this caused and measurements restarted. On the 25th and 26th of November another bad storm crossed the west of England resulting in further instrumental failure. Numerous attempts were made to fix the instrument but after various testing and liaison with Agilent, the instrument manufacturers, at the end of December 2012 it was decided that the ECD had been badly damaged and needed replacement. A contract was immediately set up for this process, however as the ECD is a radioactive source its shipment is a lengthy process. The new ECD arrived at Bristol University on the 21st of January. The heavy snowfall during this week meant that the site was inaccessible due to its elevation and road access. The replacement ECD is scheduled to be installed by an Agilent engineer on the 4th of February. This will hopefully rectify the instrumental problems and N_2O and SF_6 measurements can then continue.

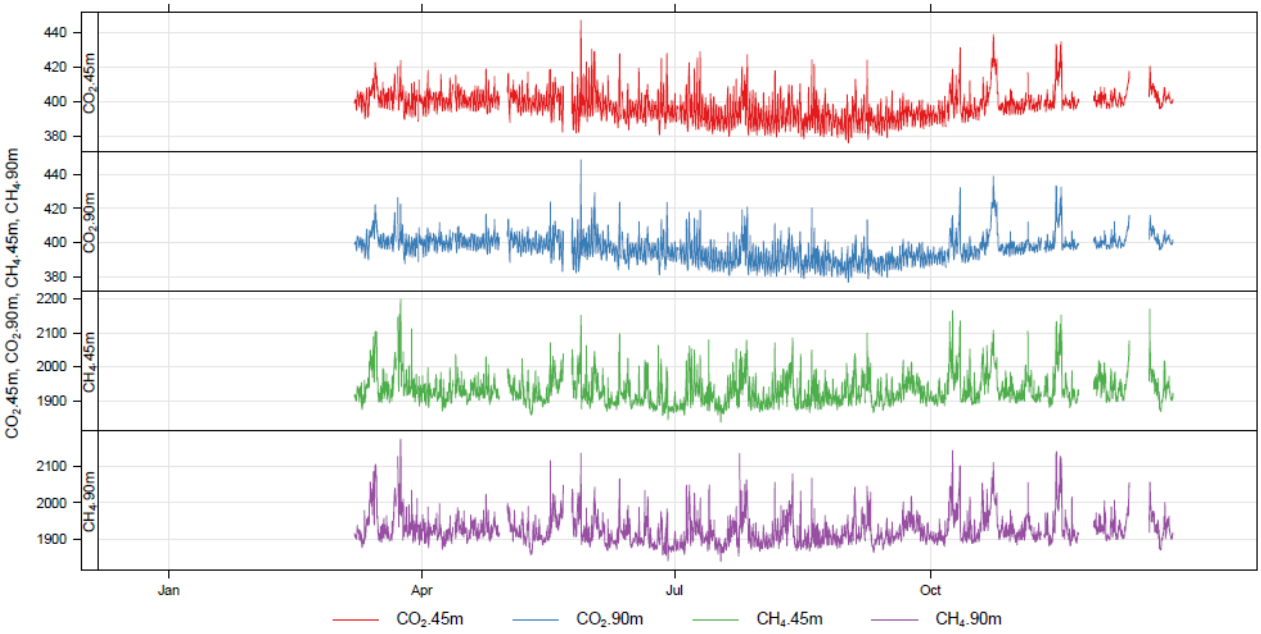

Figure 4: Ridge Hill data during 2012 for CO_2 (reported in ppm) and CH_4 (reported in ppb) at the 90 m and 45 m sampling heights.

5 Atmospheric Northern Hemisphere Baseline Trends

5.1 Introduction

This report presents the results of the analysis of the baseline concentrations of the Mace Head observations from 1990-2012 inclusive. Baseline concentrations are defined here as those that have not been influenced by significant emissions within ten days of the travel, i.e. those that are well mixed and are representative of the mid-latitude Northern Hemisphere background concentrations.

The observations at Mace Head from 1989 to December 2012 have been analysed for each gas measured. The principle tool used to estimate the baseline concentrations is the NAME dispersion model. The methodology used is presented first followed by the analysis of each individual gas. The analysis considers the long term trend of the monthly and annual baseline concentrations, their rate of growth and their seasonal cycle.

5.2 Methodology

This section describes in detail how the monthly baseline concentrations for each gas observed at Mace Head were derived. There are several specific stages to the process and the section is broken down into these segments with examples were possible.

The NAME model is run in backwards mode to estimate the recent history (30 days) of the air en-route to Mace Head. An air history map, such as those shown in figure 5, has been calculated for each 2-hour period from 2003 until Dec. 2012 using UM meteorology and from 1989-2002 using ERA-Interim meteorology, amounting to more than 100000 maps. The model output estimates the 30-day time-integrated air concentration (dosage) at each grid box (40 km horizontal resolution and 0-100m above ground level) from a release of 1 g/s at Mace Head (the receptor). The model is 3-D therefore it is not just surface transport that is modelled, an air parcel can travel from the surface to a high altitude and then back to the surface but only those times when the air parcel is within the lowest 100m above the ground will it be recorded in the maps. The computational domain covers 100^{o}W to 45.125^{o}E longitude and 10^{o}N to 80.125^{o}N latitude and extends to more than 10km vertically (actual height varies depending on version of meteorology used). For each 2-hour period 40,000 inert model particles were used to describe the dispersion. No chemical or deposition processes were modelled, this is realistic given the long atmospheric lifetimes of the vast majority of gases considered.

By dividing the dosage (gs/m^3) by the total mass emitted (3600s/hr x 2hr x 1g/s) and multiplying by the geographical area of each grid box (m^2), the model output is converted into a dilution matrix (s/m). Each element of this matrix *D* dilutes a continuous emission (*e*) of 1 g/m^{2}s from a given grid box over the previous 30 days to an air concentration (g/m^3) at the receptor (*o*) during a 2-hour period.

$$D\,\underline{e} = \underline{o} \qquad \ldots 1$$

Baseline concentrations are defined here as those that have not been influenced by significant emissions within the previous 30-days of travel en-route to Mace Head, i.e. those that are well mixed and are representative of the mid-latitude Northern Hemisphere background concentrations.

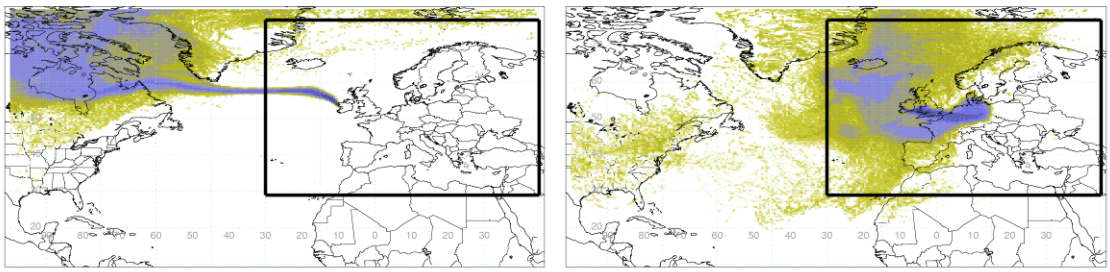

(a) (b)

Figure 5: Examples of 2-hour air history maps derived from NAME (a) baseline period (b) regionally polluted period. The air-history maps describe which surface areas (defined as within 100 m of the surface) in the previous 30-days impact the observation point at a particular time.

A 2-hour period is classed as 'baseline' if it meets the following criteria:

- The total air concentration from the nine grid boxes centred on and surrounding Mace Head is less than ten times the *dilution sensitivity limit* i.e. local emissions do not significantly contribute.
- The total air concentration contribution from a population map is less than an arbitrary limit. The limit is set so that it is clear that populated regions have not significantly contributed.
- The contribution from the southerly latitudes (south of 28° latitude) is (arbitrarily) less than twice the *dilution sensitivity limit* indicating that southerly latitude air is not significantly present.

In order to define a *dilution sensitivity limit* it is necessary to arbitrarily decide on a level of emission that would produce an agreed response at the observation point. In this study we chose an emission of 100 kt CH_4 /yr/grid to produce a 10 ppb impact. As shown later, 10 ppb is approximately the noise found in the baseline signal for methane and an emission of 100 kt/year is about 4% of the estimated UK release of methane in 2006. 10 ppb CH_4 is equivalent to ~7 ug/m3. Assuming a horizontal grid resolution of 40 km at a latitude of 50° N, 100 kt CH_4 /yr/grid is approximately ~2 ug/m^2/s, thus the *dilution sensitivity limit* is calculated, using equation 1, to be 3.4 s/m (~2.2e-9 s/m^3 at Mace Head).

The *dilution sensitivity limit* is attempting to define a threshold above which an emission source would generate a concentration at Mace Head that would be discernible above the baseline noise. The same limit value is used for all of the gases analysed. The chosen limit is arbitrary but the impact of doubling it is small.

Figure 6 shows a three month extract of the methane observations measured at Mace Head. The observations have been colour coded to indicate whether, using the above classification, the air mass they were sampled from was considered baseline. For the baseline analysis all non-baseline observations are removed.

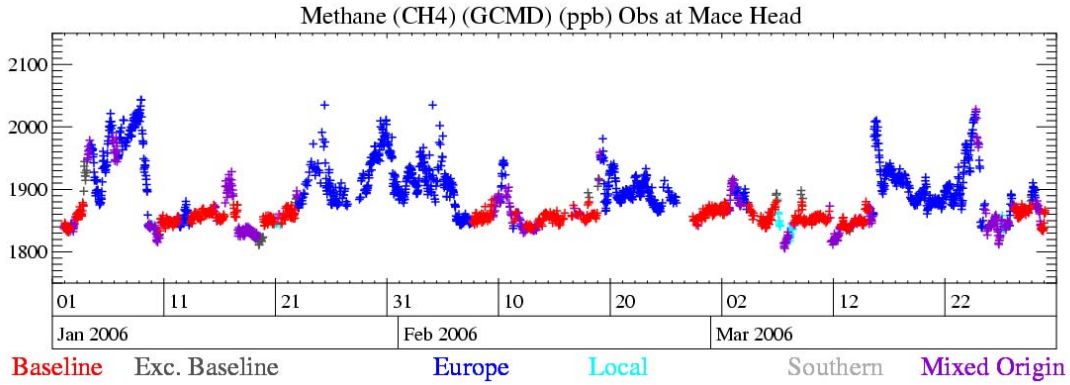

Figure 6: 3-month time-series of Mace Head methane observations showing the impact of the baseline and non-baseline classification. The baseline observations are shown in red.

The points defined as baseline using the above methodology still have a certain level of noise. The principle reasons for this are; unexpected short-lived emissions e.g. forest fires in Canada or from shipping, local emissions that are not identified using the above criteria above, incorrectly modelled meteorology or transport, i.e. European air defined as baseline by error.

Irrespective of the methodology used to identify these events some will inevitably be classed as baseline when it is inappropriate to do so. To capture such events the baseline data are statistically filtered to isolate and remove these non-baseline observations. For each baseline point in turn, the baseline points in a 40-day window surrounding this central value are considered and, provided that there are sufficient points (>11 with at least 4 in each third of the window or more than 18 in two thirds), a quadratic is fitted to these values. The standard deviation of the actual points and the fitted curve is calculated (*std*) and if the current baseline value is more than *x std* away from the fitted value it is marked for exclusion from the baseline observations. After all baseline points have been considered, those to be excluded are removed. The process is repeated nine times, each time the value for *x* is gradually reduced from 6 to 2, thus ensuring that those points statistically far from the fitted baseline do not unduly affect the points to be excluded by skewing the fitted curve. If there are insufficient baseline points in a 40 day window the values are only included if the spread in the points is small and there are at least 5. The observations removed through this statistical filter are shown in black in figure 6.

For each hour in the time-series the baseline points in a running 40-day window are fitted using a quadratic function and the value extracted for the current hour in question. The process is then advanced by an hour and repeated. If there are insufficient baseline points well spaced within the window (at least 3 in each quarter) it is gradually extended up to 150-days.

For each hour within the observation time record a smoothed baseline concentration is estimated by taking the median of all fitted baseline values within a 20-day time window. If there are fewer than 72 baseline values in the time window then the window is steadily increased up to a maximum of 40 days. If there are still insufficient points then no smoothed baseline concentration is estimated for that hour.

The noise or potential error in the smoothed baseline concentration is estimated to be the standard deviation of the difference between the observations classed as baseline and the smoothed baseline concentrations at the corresponding times. Figure 7 shows, on a much expanded y-axis compared to figure 6, the typical spread of baseline observations about the smoothed continuous baseline estimate.

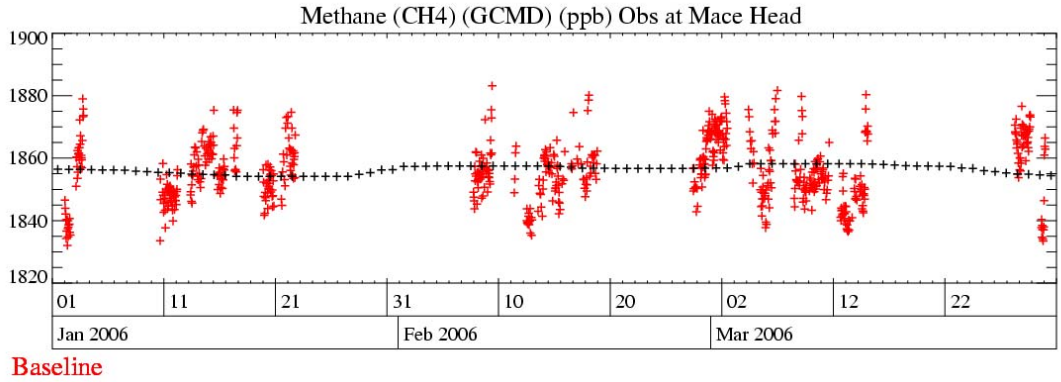

Figure 7: Observations of methane at Mace Head within a 3-month period classed as baseline (red) with the estimated daily baseline concentrations for the same period (black). Note: the y-axis has been expanded compared to figure 6.

The hourly baseline concentrations are split into two components, a long-term trend and a residual component (seasonal cycle). Two methods have been used:

Kolmogorov–Zurbenko method

Kolmogorov–Zurbenko (KZ) filter involves *k* time iterations of a moving average of a given time duration and is ideally suited to this type of problem. For this application the length of the moving average window was set to one year and the number of iterations was set to four. With these parameters a 12-month moving average was applied to the data four times, thereby approximately removing wavelengths smaller than 2-years. At each hour in the time-series calculate the 12-month average of the baseline mass mixing ratios centred on this hour. This is the long-term trend component, subtracting this from the actual hourly baseline estimate at this time gives the residual.

3-year quadratic method

At each hour calculate the 12-month average centred on this hour (y_a). For the three year period centred on this hour calculate the quadratic line using standard value decomposition, that best-fits or minimises the

difference between the computed time-series and y_a. This is the long-term trend component, subtracting this from the actual hourly baseline estimate at this time gives the residual.

Monthly and annual baseline concentrations are estimated by averaging all of the long-term trend daily baseline values within the appropriate time window. A monthly value is estimated if there are at least 21 daily values within the month, this ensures a good representation of the whole month. An annual value is estimated if there are at least 330 daily values within the calendar year, ensuring a good representation of the whole year.

The annual growth rate on a particular day is defined as the local slope of the long-term trend on that day. The local slope is estimated by linearly fitting a best-fit line through the trend concentration values for the day before, current day and day after. Monthly averages of these growth rates for methane and nitrous oxide are shown in figures 22 and 24.

The daily residual concentration values are averaged for each month over the data period studied to produce a seasonal cycle. The mean seasonal cycles of the principle GHG gases are shown in section 5.3. The range of values for each month is also shown, along with the first, middle and last individual year seasonal cycles.

5.3 Baseline Concentrations

For each gas observed at Mace Head a baseline analysis has been performed. ECMWF meteorology is used from 1989 – 2002 inclusive and Met Office meteorology from 2003-2012 inclusive. The figures that follow illustrate for each gas the monthly and annual baselines, the changing baseline growth rates and the average seasonal cycle seen within the observations. The gases are grouped into similar chemical families; CFC, HCFC, HFC, fluorine compounds (PFCs), chlorine compounds, bromine compounds (halons), hydrocarbons, oxides of carbon and finally nitrous oxide, ozone and hydrogen. Table 1 summaries the annual baseline mass mixing ratios within the observation period for each of the gases considered.

The baseline trends, growth rates and seasonal cycles are presented for the principle GHGs, notably, HFCs, PFCs, SF_6, CO_2, CH_4 and N_2O. Please refer to the website www.metoffice.gov.uk/atmospheric-trends for the presentation of all of the gases analysed.

Gas	1990	1991	1992	1993	1994	1995	1996	1997	1998	1999
CFC-11 (GCMD)	264	267	268	269	268	267	266	264	263	261
CFC-12 (GCMD)	496	506	517	522	529	533	537	540	542	544
CFC-13										
CFC-113 (GCMD)	75.5	81.1	84.2	85	84.6	84.6	84.3	83.8	83.2	82.7
CFC-113										
CFC-115										8
HCFC-124										1.3
HCFC-141b						5.1	7.3		11.3	13.3
HCFC-142b						8	9.2	10.7	11.4	12.4
HCFC-22										145
HFC-125										1.3
HFC-134a						2.3	4.3	6.3	9.6	13.4
HFC-143a										
HFC-152a						1.2	1.2	1.3	1.9	2.2
HFC-23										
HFC-32										
HFC-227ea										
HFC-236fa										
HFC-245fa										
HFC-365mfc										
PFC-14										
PFC-116										
PFC-218										
SF6										
SO2F2										
CH3Cl										535
CH2Cl2							36.3	36.1	35	31.8
CHCl3 (GCMD)						12.6	13	12.1	12.2	11.6
CHCl3							12.5	12	12.6	12.7
CH3CCl3 (GCMD)	151	152	150	139	125	111	95	80	66	55
CH3CCl3										
CCl4 (GCMD)			105	104	103	102	101	100	99	98
CHClCCl2										
CCl2CCl2										
CH3Br										11
Halon-1211						3.5	3.6		4	4.2
Halon-1301										2.8
Halon-2402										
CH2Br2										
CHBr3										
CH3I										
CH4 (ppb)	1792	1812	1804	1815	1818	1822	1827	1826	1836	1841
C2H6										
C6H6										
CO (ppb)						119	130	118	145	124
CO2 (ppm)				357	359	361	363	364	367	369
N2O (ppb)	309	310	310	311	312	312	313	314	314	315
O3 (ppb)	34.8	35.8	34.5	34.6	36.3	34.5	36.9	36.6	39.4	41.7
H2 (ppb)						496	502	494	507	507

Table 1: Annual Northern hemisphere baseline mass mixing ratios for all gases measured at Mace Head 1990-1999 (ppt unless stated).

Gas	2000	2001	2002	2003	2004	2005	2006	2007	2008	2009
CFC-11 (GCMD)	260	259	256	255	253	250	248	246	244	243
CFC-12 (GCMD)	546	546	546	546	545	544	543	541	539	536
CFC-13					2.8	2.8			2.9	2.9
CFC-113 (GCMD)	82.2	81.5	80.6	79.9	79.3	78.7	77.8	77.1	76.6	76
CFC-113						78.8	77.9		76.7	76
CFC-115	8.1	8.2	8.1	8.2	8.4	8.4	8.4	8.4	8.4	8.4
HCFC-124	1.4	1.6	1.6	1.6	1.6	1.6	1.6	1.6	1.6	1.6
HCFC-141b	15.2	16.4	17.6	18.6	19.1	19.1	19.6	20.2	20.9	21.3
HCFC-142b	13.6	14.6	15	15.5	16.2	17	18.1	19.3	20.6	21.4
HCFC-22	151	158	164	169	175	180	187	195	204	212
HFC-125	1.6	2.1	2.4	3.1	3.7	4.3	5	5.8	6.9	8
HFC-134a	17.2	20.8	25	29.6	34.7	39.3	43.8	47.9	53.3	58
HFC-143a					5.5	6.4	7.4	8.4	9.6	10.7
HFC-152a	2.5	2.9	3.4	4.2	4.8	5.6	6.8	7.9	8.8	8.9
HFC-23									22.5	23
HFC-32					1.1	1.6	2.1	2.7	3.4	4.1
HFC-227ea								0.4	0.5	0.6
HFC-236fa								0.1	0.1	0.1
HFC-245fa								0.9	1.1	1.2
HFC-365mfc					0.2	0.3	0.4	0.5	0.5	0.6
PFC-14					74.9	75.5	76.2	76.9	77.7	78.1
PFC-116					3.6	3.7	3.8	3.9	4	4.1
PFC-218					0.4	0.5	0.5	0.5	0.5	0.5
SF6					5.6	5.8	6.1	6.3	6.6	6.9
SO2F2						1.5	1.5	1.6	1.6	1.7
CH3Cl	521	514	514	524	522	529	523	530	535	532
CH2Cl2	30.4	29.3	29.4	31.2	31	30.7	32.5	34.4	36.3	36.6
CHCl3 (GCMD)	11.1	11.1	11.2	11.4	11.4	11.3	11.4	11.4	11.5	11
CHCl3	11.6	10.9	10.4	11	10.8	11.1	11.1	10.6	10.6	10.2
CH3CCl3 (GCMD)	46	39	32	27	23	19	16	13	11	9
CH3CCl3		39.3	31.1	26.7	23.1	18.8	15.7	13.1	11	9.3
CCl4 (GCMD)	97	96	95	94	93	92	91	90	89	88
CHClCCl2	1.4	1.4	1.4	1.3	1.6	1	1	1.1	0.7	0.6
CCl2CCl2		5.1	4.7	4.8	4.7	3.9	3.8	3.6	3.4	3
CH3Br	10.5	9.9	9.1	8.9	9.1	9.9	9.5	9.1	9.2	8.6
Halon-1211	4.3	4.4	4.4	4.4	4.5	4.5	4.5	4.4	4.4	4.3
Halon-1301	2.9	3	3	3.1	3.1	3.2	3.2	3.2	3.3	3.3
Halon-2402						0.5	0.5	0.5	0.5	0.5
CH2Br2							1.6	1.7	1.6	1.6
CHBr3						5.7	6	4.8	4.8	4.9
CH3I		1.5	1.6	1.7	2	2	1.4	1.6	1.4	1
CH4 (ppb)	1842	1843	1844	1854	1848	1847	1847	1855	1864	1868
C2H6						1272	1300	1338	1339	1068
C6H6						66.3	64.2	61.8	65.7	61.7
CO (ppb)	119	117	127	137	123	123	123	120	120	114
CO2 (ppm)	369	371	373	375	378	379	382	384	386	387
N2O (ppb)	316	317	318	318	319	320	320	321	322	323
O3 (ppb)	40.1	39.4	39.8	40.7	40.3	39.6	40.8	39.5	40.5	39.9
H2 (ppb)	499	495	497	500	497	500	504	499	502	498

Table 2: Annual Northern hemisphere baseline mass mixing ratios for all gases measured at Mace Head 2000-2011 (ppt unless stated).

Gas	2010	2011	2012	Avg Growth	Avg Growth 12 months
CFC-11 (GCMD)	241	238	236	-1.17	-2.2
CFC-12 (GCMD)	533	531	528	1.68	-2.71
CFC-13	2.9	3	3	0.02	0.03
CFC-113 (GCMD)	75.3	74.9	74.3	0.04	-0.32
CFC-113	75.2	74.5	74	-0.68	-0.56
CFC-115	8.4	8.4	8.4	0.04	0.02
HCFC-124	1.5	1.4	1.4	0.02	-0.05
HCFC-141b	22	23.1	24.1	0.89	1.14
HCFC-142b	21.9	22.7	23	0.9	0.59
HCFC-22	219	226	231	6.72	5.46
HFC-125	9.2	10.8	12.4	0.81	1.59
HFC-134a	63.4	68.4	73.4	4.2	4.9
HFC-143a	11.9	13.2	14.5	1.13	1.31
HFC-152a	9.4	10	10.1	0.55	0.36
HFC-23	23.7	24.7	25.5	0.75	0.94
HFC-32	5.2	6.5	7.7	0.82	1.26
HFC-227ea	0.6	0.7	0.8	0.07	0.07
HFC-236fa	0.1	0.1	0.1	0.01	0.01
HFC-245fa	1.3	1.5	1.7	0.15	0.19
HFC-365mfc	0.6	0.7	0.8	0.08	0.08
PFC-14	78.7	79.5	80.3	0.68	0.79
PFC-116	4.1	4.2	4.3	0.08	0.08
PFC-218	0.6	0.6	0.6	0.02	0.02
SF6	7.2	7.5	7.8	0.28	0.3
SO2F2	1.7	1.8	1.9	0.06	0.09
CH3Cl	531	521	528	-1.83	-3.59
CH2Cl2	40.2	39.7	41.9	0.24	-0.15
CHCl3 (GCMD)	12	11.6	11.7	-0.06	-0.19
CHCl3	11.2	10.9	10.9	-0.09	-0.14
CH3CCl3 (GCMD)	8	7	5	-6.56	-1.2
CH3CCl3	7.8	6.5	5.4	-3.03	-1.22
CCl4 (GCMD)	87	86	85	-0.99	-0.9
CHClCCl2	0.5	0.4	0.3	-0.09	-0.14
CCl2CCl2	3	2.7	2.5	-0.23	-0.31
CH3Br	8.3	8.4	8.3	-0.21	0.01
Halon-1211	4.2	4.2	4.1	0	-0.08
Halon-1301	3.3	3.3	3.3	0.04	0.03
Halon-2402	0.5	0.5	0.5	-0.01	0
CH2Br2	1.8	1.6	1.7	0	-0.08
CHBr3	5.6	4.5	4.5	-0.25	-0.63
CH3I	1	1	0.9	-0.07	-0.12
CH4 (ppb)	1872	1875	1882	4.11	5.29
C2H6	1068			-62.4	-144.4
C6H6	61.9			-1.12	-1.51
CO (ppb)	122	116	124	0.05	-1.33
CO2 (ppm)	390	392		1.93	2.09
N2O (ppb)	323	324	325	0.72	0.97
O3 (ppb)	39	39.6	39.9	0.22	0.02
H2 (ppb)	498	504	505	0.56	3.31

Table 3: Annual Northern hemisphere baseline mass mixing ratios for all gases measured at Mace Head 2010-2012 (ppt unless stated) and Northern hemisphere baseline growth rates for all gases measured at Mace Head (ppt/yr unless stated): all years (first column) and current (last column).

5.3.1 HFCs

Hydrofluorocarbos (HFCs) are replacement chemicals for the long-lived ozone depleting substances in various applications such as refrigeration, fire extinguishers, propellants, and foam blowing. The most recent measurements of the HFCs at Mace Head indicate that the mixing ratios of all HFC compounds continue to grow, as is consistent with sustained emissions of these replacement compounds into the atmosphere. The baseline monthly mean, mixing ratios for all the HFCs are shown in figures 8-17 and the growth rates of these compounds, calculated from the data, are presented in Table1c.

HFC-125 (CHF_2CF_3): This compound is used in refrigeration blends and for fire suppression. It has a GWP_{100} of 3500 and an atmospheric lifetime of 13.4 years. (O'Doherty et al., 2009). This compound is growing rapidly in the atmosphere reaching a level of 13.5 ppt in Dec. 2011 with a current growth rate of 1.6 ppt/yr.

HFC-134a (CH_2FCF_3): Globally HFC-134a is the most abundant HFC present in the atmosphere, used predominantly in refrigeration and mobile air conditioning (MAC). Due to its long lifetime, 13.4 years, and relatively high GWP_{100} 1370 (Forster et al., 2007), the use of HFC-134a (and any other HFCs with a GWP_{100} >150) will be phased out in Europe between 2011 and 2017. It is proposed that a very gradual phase-out of the use of HFC-134a in cars will also take place outside Europe because of the global nature of the car industry. However in developing countries the potential for growth of HFC-134a is still large (Velders et al., 2009). As of December 2012 the atmospheric mole fraction of HFC-134a was 76.7 ppt and recent growth is estimated to be 4.9 ppt/yr.

HFC-143a (CH_3CF_3) is used mainly in refrigerant blends. In December 2012 it reached levels of 15.3 ppt. These levels have increased dramatically from the low levels in 1997 with an increasing growth rate, currently estimated to be 1.3 ppt/yr. It has a relatively long atmospheric lifetime of 47.1 years

HFC-152a (CH_3CHF_2) has a relatively short lifetime of 1.5 years due to its efficient removal by OH oxidation in the troposphere, consequently it has the smallest GWP_{100} at 133, of all of the major HFCs. It is used as a foam-blowing agent and aerosol propellant, and given its short lifetime has exhibited substantial growth in the atmosphere since measurement began in 1994. However, in the last few years the rate of growth has slowed somewhat to ~0.4 ppt/yr, reaching a mixing ratio in Dec 2011 of 10.7 ppt.

HFC-23 (CHF_3) is primarily a by-product formed during the production of HCFC-22. For this reason it has grown at an average rate of 0.8 ppt/yr and by December 2012 had reached a mixing ratio of 26.1 ppt. It is the second most abundant HFC in the atmosphere after HFC-134a, this combined with a long atmospheric lifetime of 222 years makes this compound a potent GHG. Emissions of HFC-23 in developed countries has declined due to the Montreal Protocol phase-out schedule for HCFC-22, however, emissions from developing countries (despite the implementation of HFC-23 incineration through the Clean Development Mechanism) continues to drive global mixing ratios up.

Three new HFC compounds have now successfully been added to the Medusa analysis (since 11 January 2008). The atmospheric mole fraction of HFC-245fa in December 2012 was 1.9 ppt and it is growing at a rate of 0.19 ppt/yr. This compounds is used as a foam blowing agent for polyurethane (PUR) foams (atmospheric lifetime 7.6 years and GWP_{100} of 1020). HFC-227ea is used as a propellant for medical aerosols and a fire fighting agent (atmospheric lifetime 34.2 years and GWP_{100} of 3140). It is has reached a mole fraction of 0.86 ppt with a growth rate of 0.07 ppt/yr. Finally, HFC-236fa, used as a fire fighting agent, (atmospheric lifetime 240 years and GWP_{100} of 9500) has reached a mixing ratio of 0.10 ppt and is growing at a rate of 0.01 ppt/yr.

5.3.1.1 HFC-125

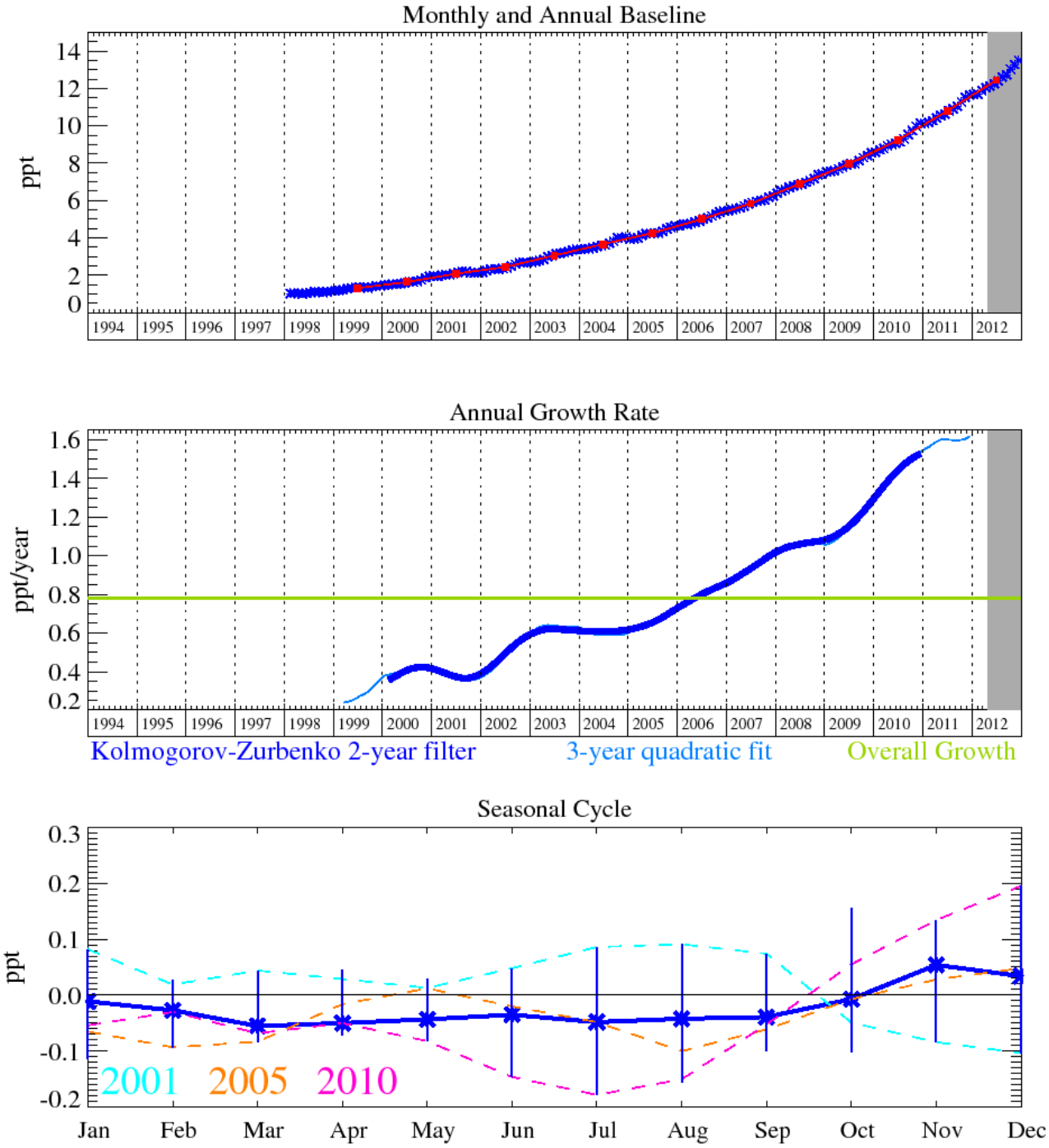

HFC-125 (CHF_2CF_3) is most commonly used in refrigeration blends and for fire suppression. It has an RE of 0.23 W m^{-2} ppb^{-1}, a lifetime of 28.2 years and a GWP_{100} of 3,420.

The grey area on each plot contains data that are unratified and therefore provisional.

Figure 8: HFC-125: Monthly (blue) and annual (red) baseline concentrations (top plot). Annual (blue) and overall average growth rate (green) (middle plot). Seasonal cycle (de-trended) with year to year variability (lower plot).

5.3.1.2 HFC-134a

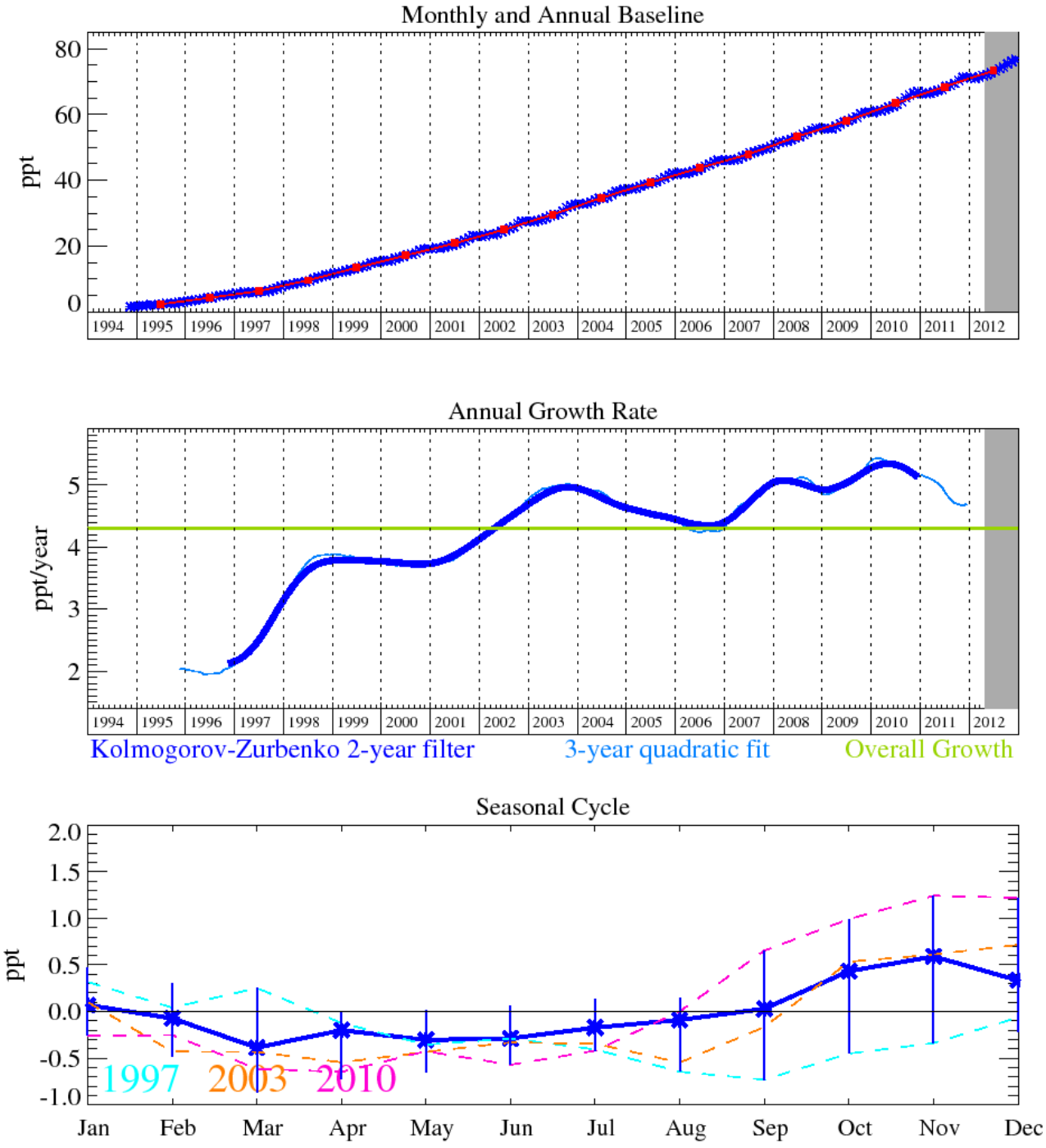

HFC-134a (CH_2FCF_3) is currently the most common HFC in the atmosphere. It is primarily used as a refrigerant for air conditioning in motor vehicles. It has a GWP_{100} of 1,370 and an atmospheric lifetime of 13.4 years and is due to be phased out in Europe. It has an RE value of 0.16 W m^{-2} ppb^{-1}.

The grey area on each plot contains data that are unratified and therefore provisional.

Figure 9: HFC-134a: Monthly (blue) and annual (red) baseline concentrations(top plot). Annual (blue) and overall average growth rate (green) (middle plot). Seasonal cycle (de-trended) with year to year variability (lower plot).

5.3.1.3 HFC-143a

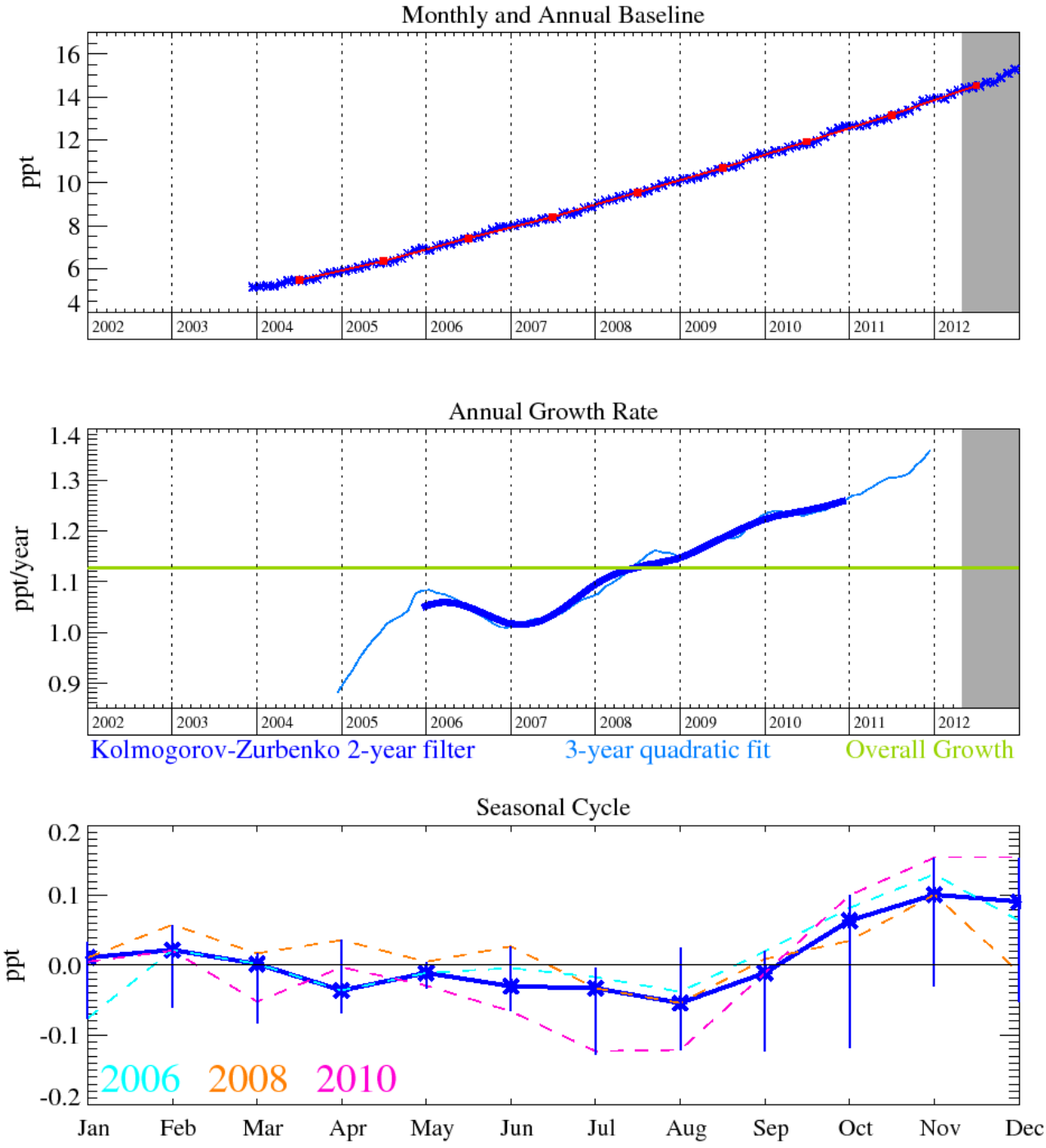

HFC-143a (CH_3CF_3) is mainly used in refrigerant blends. It has a GWP_{100} of 4,400, a lifetime of 47.1 years and an RE of 0.13 W m^{-2} ppb^{-1}.

The grey area on each plot contains data that are unratified and therefore provisional.

Figure 10: HFC-143a: Monthly (blue) and annual (red) baseline concentrations (top plot). Annual (blue) and overall average growth rate (green) (middle plot). Seasonal cycle (de-trended) with year to year variability (lower plot).

5.3.1.4 HFC-152a

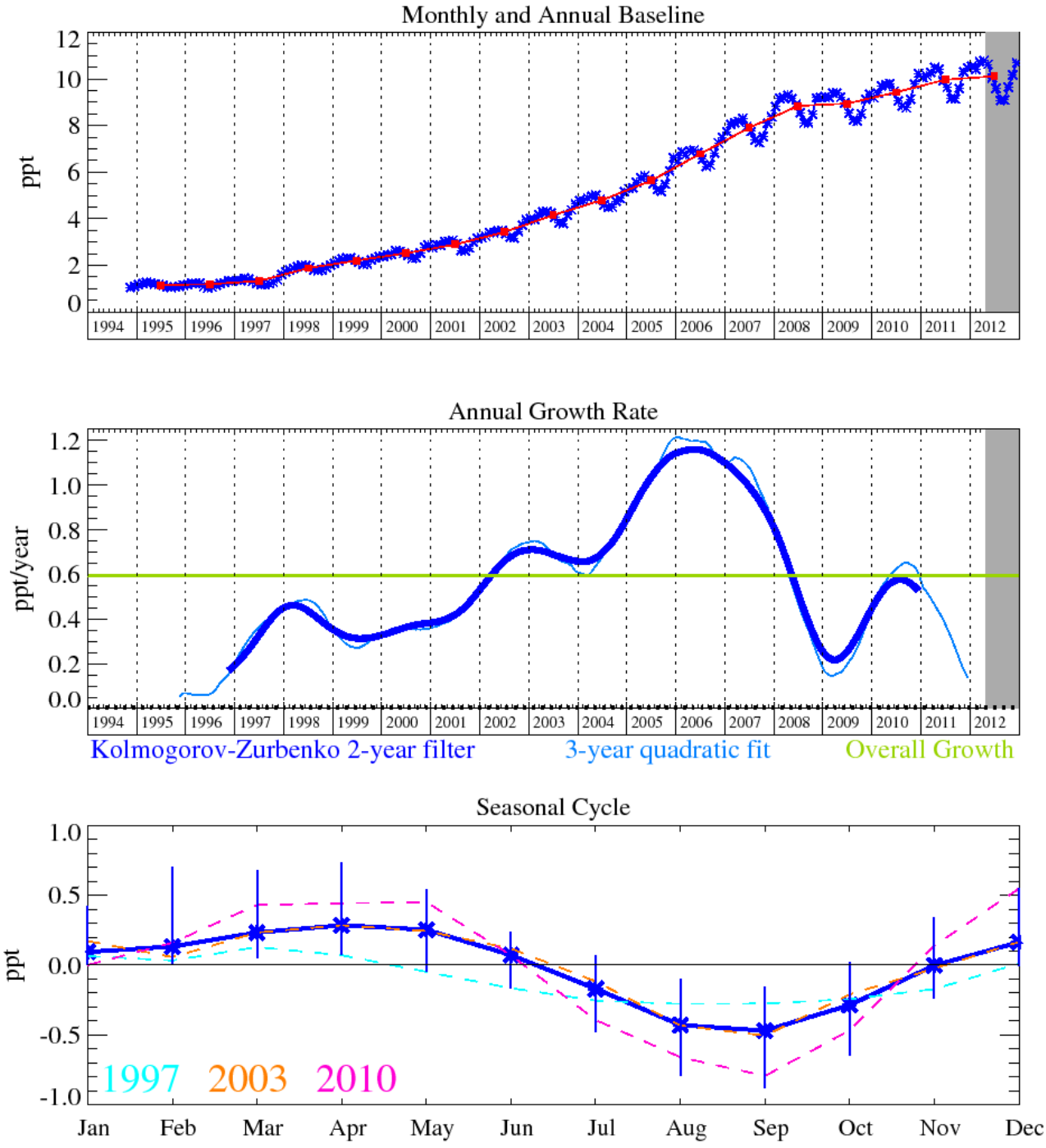

HFC-152a (CH_3CHF_2) is used as an aerosol propellant and a foam-blowing agent. It has a short lifetime of 1.5 years and the smallest GWP_{100} of all the major HFCs, 133. It has an RE of 0.09 W m^{-2} ppb^{-1}.

The grey area on each plot contains data that are unratified and therefore provisional.

Figure 11: HFC-152a: Monthly (blue) and annual (red) baseline concentrations (top plot). Annual (blue) and overall average growth rate (green) (middle plot). Seasonal cycle (de-trended) with year to year variability (lower plot).

5.3.1.5 HFC-23

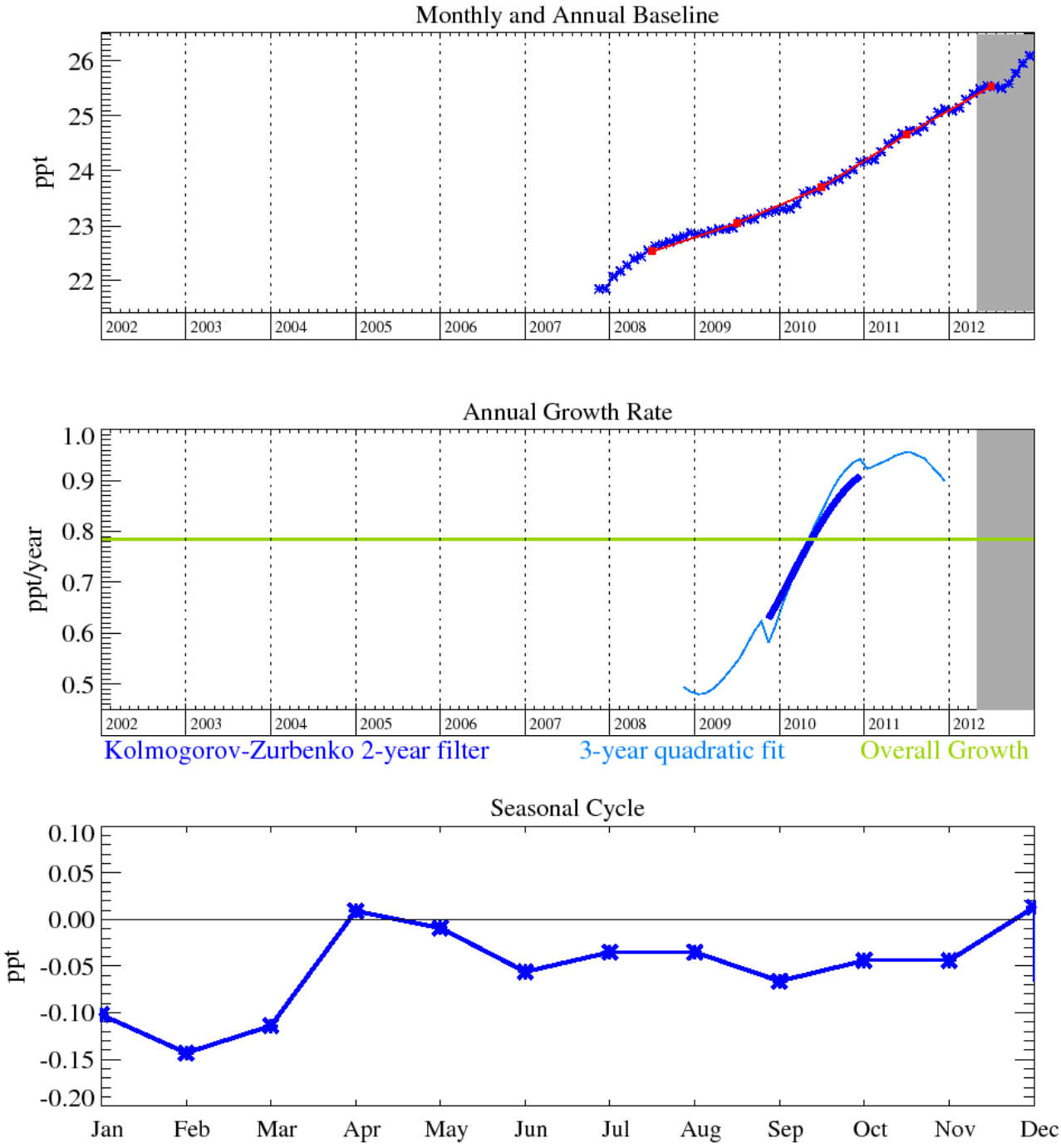

HFC-23 (CHF_3) is a by-product formed during the manufacture of HCFC-22. Other minor emissions arise from the electronic industry and fire extinguishers. HFC-23 has a GWP_{100} of 14,200 with a lifetime of 222 years. It has an RE of 0.19 W m^{-2} ppb^{-1}. An increase in HFC-23 in recent years coincides with a substantial increase in HCFC-22 production by developing countries.

The grey area on each plot contains data that are unratified and therefore provisional.

Figure 12: HFC-23: Monthly (blue) and annual (red) baseline concentrations. Annual (blue) and overall average growth rate (green) (lower plot).

5.3.1.6 HFC-32

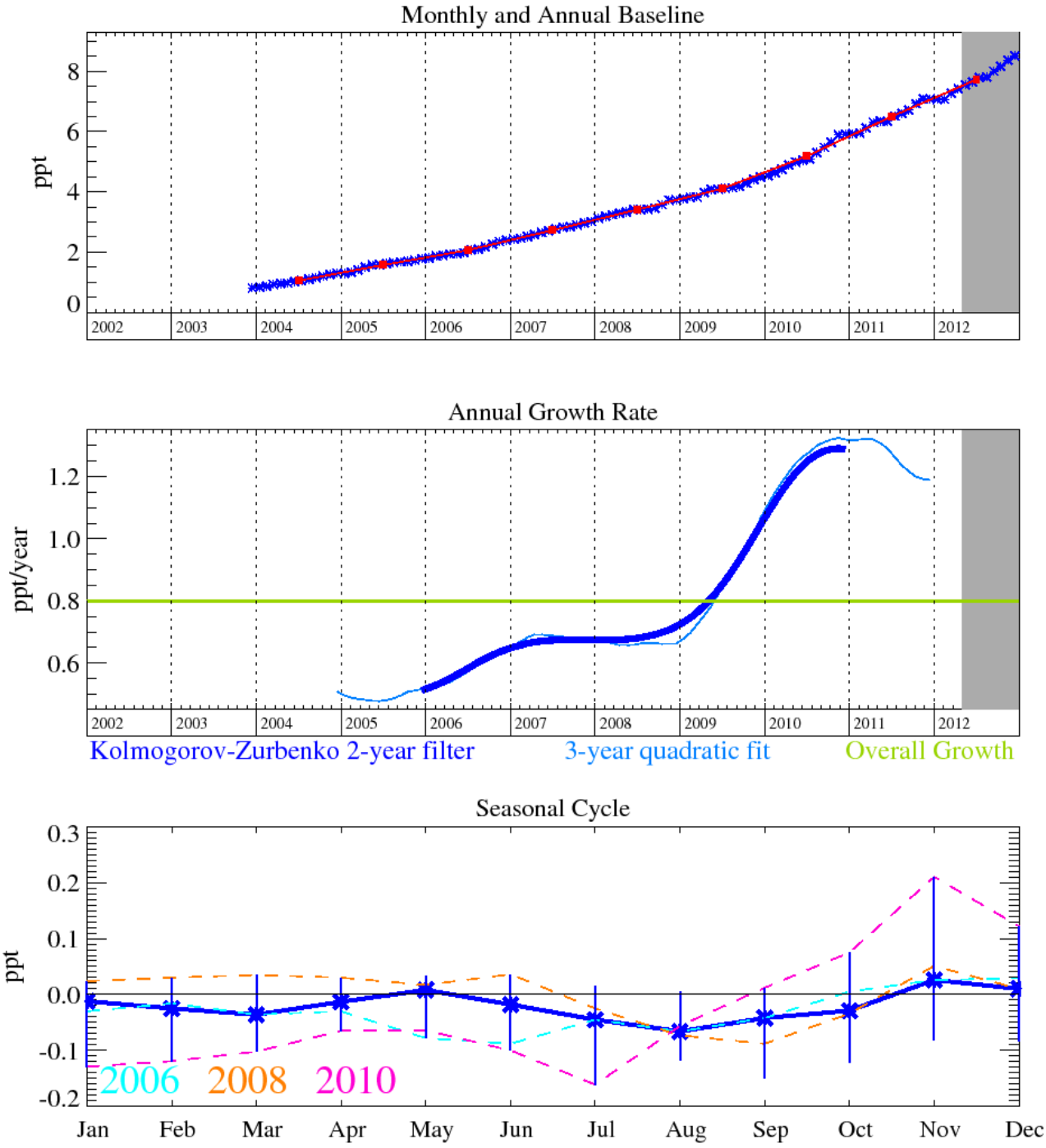

HFC-32 (CH_2F_2) is used as a blend component of refrigerants in modern air conditioning units. It has a GWP_{100} of 716, a lifetime of 5.2 years, and an RE of 0.11 W m^{-2} ppb^{-1}.

The grey area on each plot contains data that are unratified and therefore provisional.

Figure 13: HFC-32: Monthly (blue) and annual (red) baseline concentrations (top plot). Annual (blue) and overall average growth rate (green) (middle plot). Seasonal cycle (de-trended) with year to year variability (lower plot).

5.3.1.7 HFC-227ea

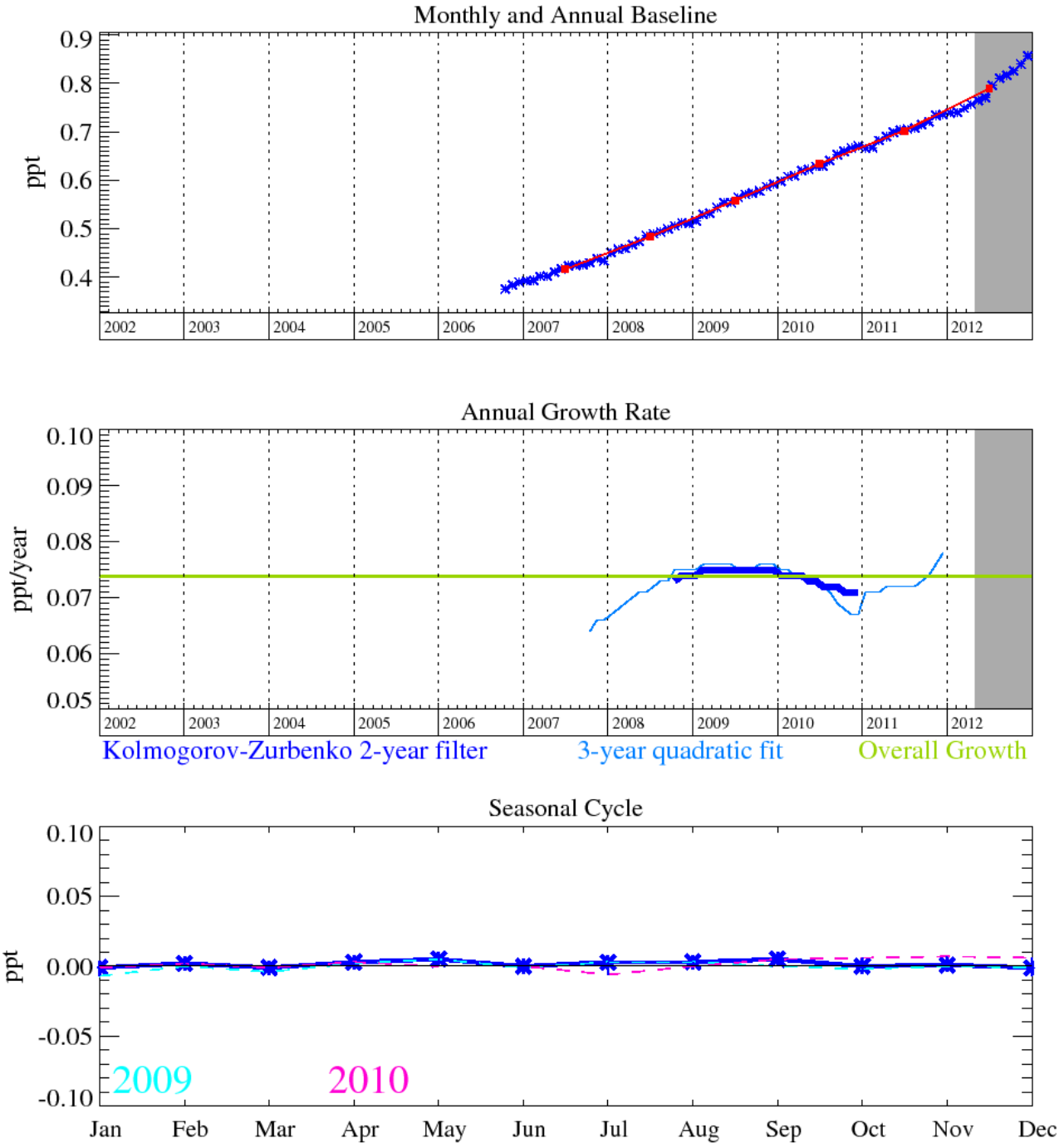

HFC-227ea (C_3HF_7) is primarily used in fire suppression but has minor roles to play in metered dose inhalers and foam blowing. It has a lifetime of 38.9 years and a relatively high RE value of 0.26 W m^{-2} ppb^{-1}. It's GWP_{100} is 3,580.

The grey area on each plot contains data that are unratified and therefore provisional.

Figure 14: HFC-227ea: Monthly (blue) and annual (red) baseline concentrations (top plot). Annual (blue) and overall average growth rate (green) (middle plot). Seasonal cycle (de-trended) with year to year variability (lower plot).

5.3.1.8 HFC-236fa

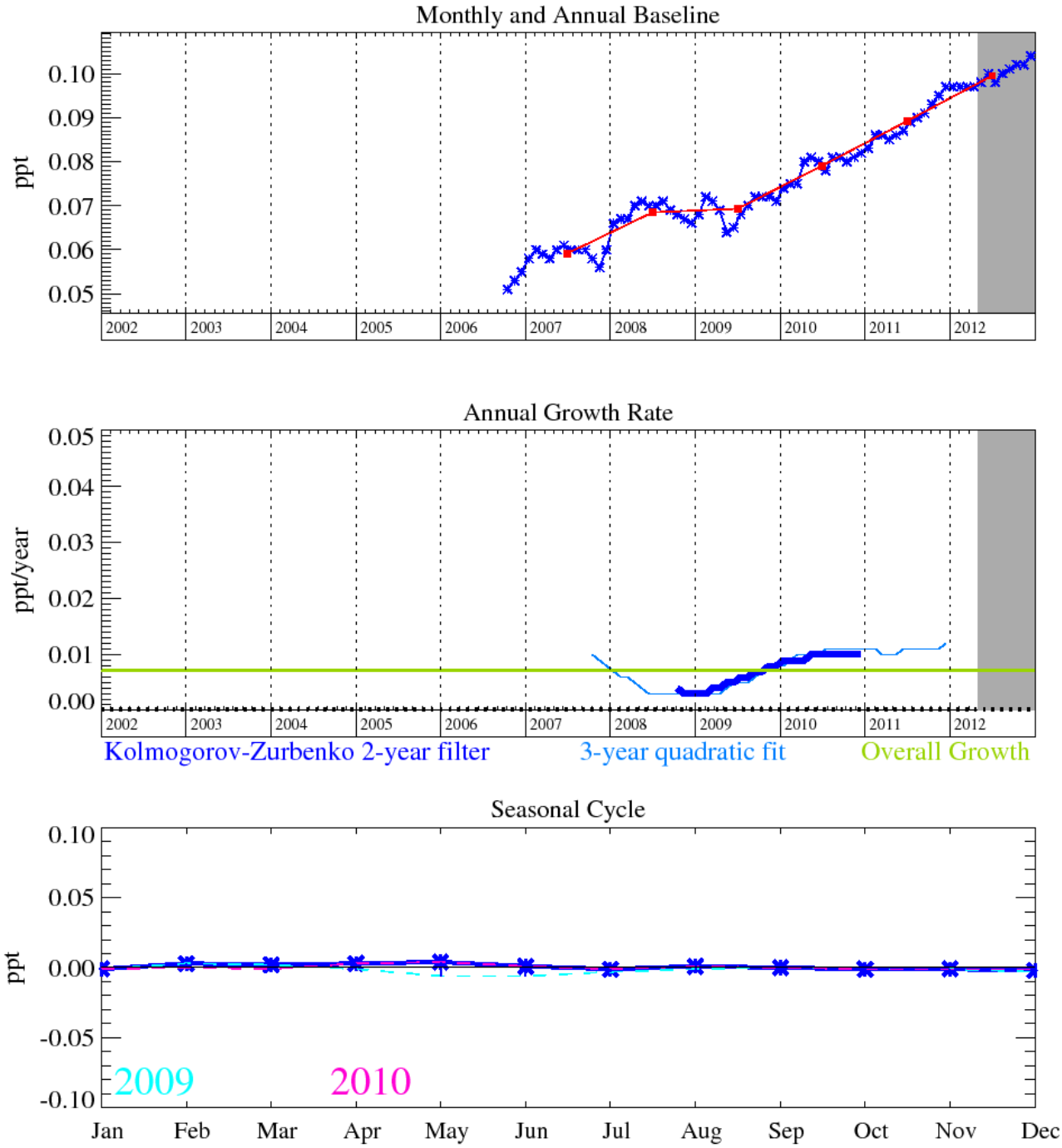

HFC-236fa ($C_3H_2F_6$) is used as a fire extinguishant and an explosion suppressing agent. It has a long lifetime of 242 years and also possesses very high RE and GWP_{100} values, 0.28 W m^{-2} ppb^{-1} and 9,820 respectively.

The grey area on each plot contains data that are unratified and therefore provisional.

Figure 15: HFC-236fa: Monthly (blue) and annual (red) baseline concentrations (top plot). Annual (blue) and overall average growth rate (green) (middle plot). Seasonal cycle (de-trended) with year to year variability (lower plot).

5.3.1.9 HFC-245fa

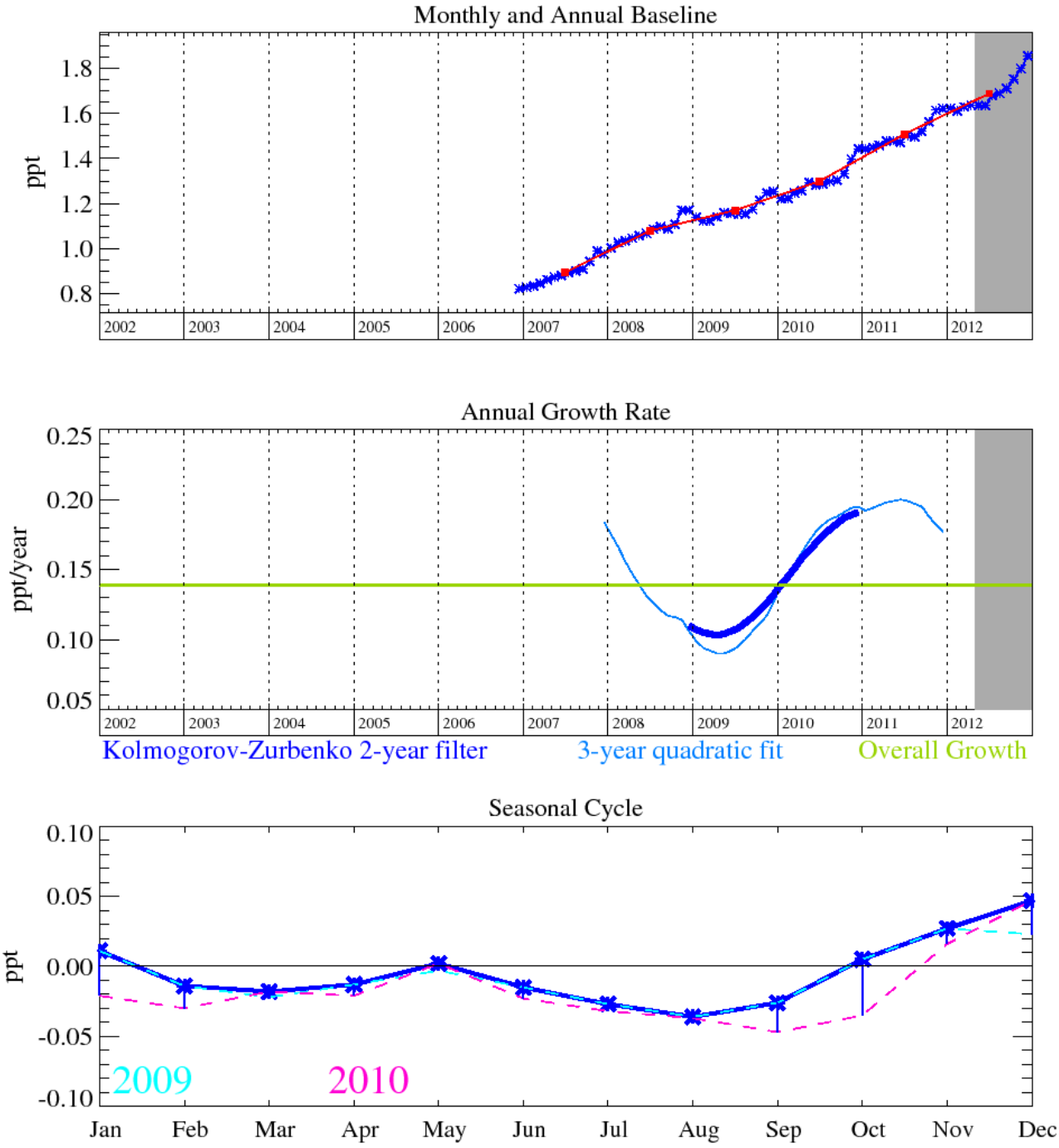

HFC-245fa ($C_3H_3F_5$) was developed for the same use as HFC-365mfc, to replace the more ozone harmful HCFC-141b as a foam blowing agent. Although it possesses a higher GWP_{100} and RE, 1,050 and 0.28 W m^{-2} ppb^{-1} respectively, it has a shorter lifetime of 7.7 years.

The grey area on each plot contains data that are unratified and therefore provisional.

Figure 16: HFC-245fa: Monthly (blue) and annual (red) baseline concentrations (top plot). Annual (blue) and overall average growth rate (green) (middle plot). Seasonal cycle (de-trended) with year to year variability (lower plot).

5.3.1.10 HFC-365mfc

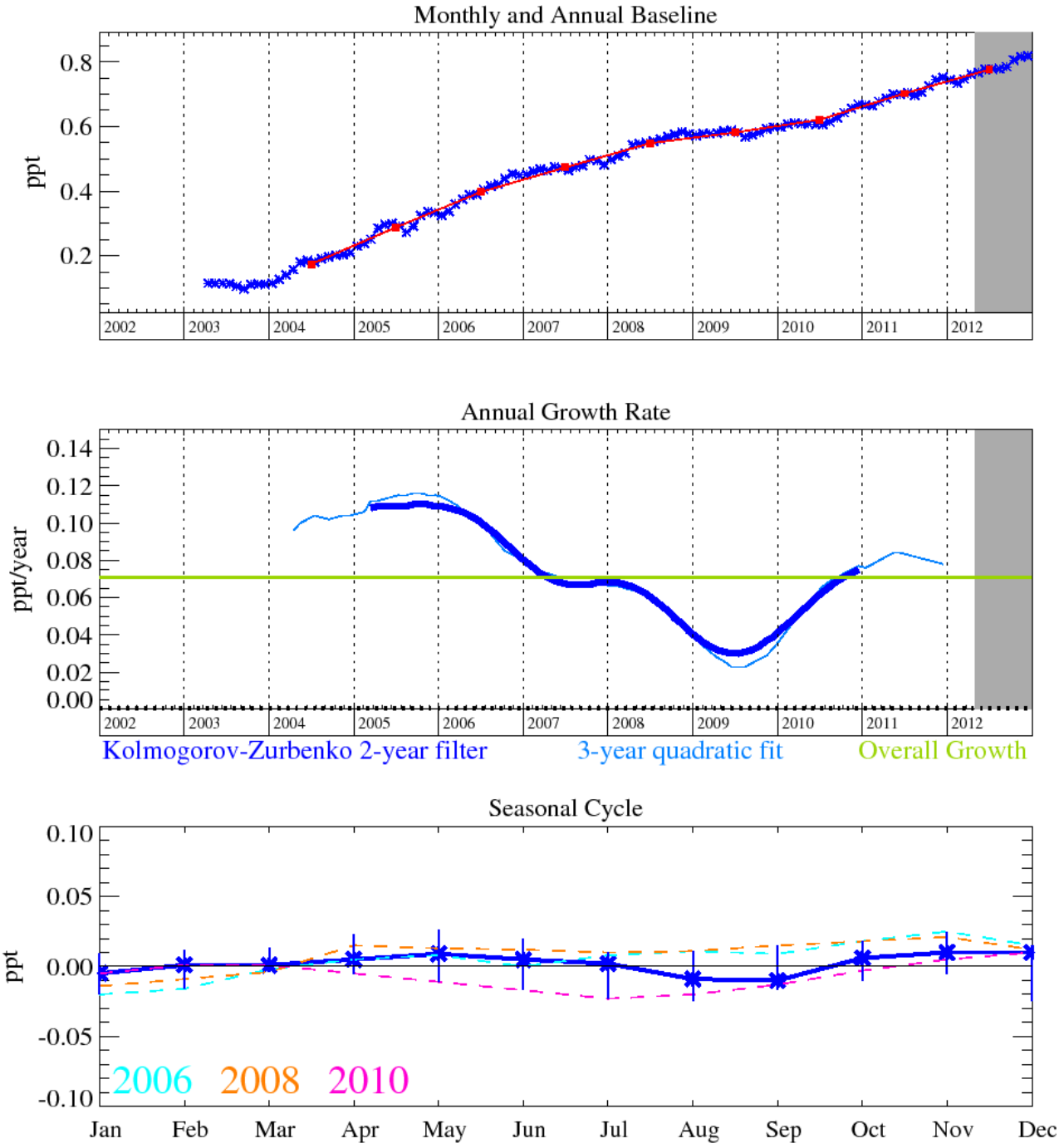

HFC-365mfc ($C_4H_5F_5$) was developed as a foam blowing replacement for HCFC-141b. It has a GWP_{100} of 842, an RE of 0.22 W m^{-2} ppb^{-1} and a lifetime of 8.7 years.

The grey area on each plot contains data that are unratified and therefore provisional.

Figure 17: HFC-365mfc: Monthly (blue) and annual (red) baseline concentrations (top plot). Annual (blue) and overall average growth rate (green) (middle plot). Seasonal cycle (de-trended) with year to year variability (lower plot).

5.3.2 Fluorine compounds

The Medusa data record for CF_4, C_2F_6, C_3F_8, and SF_6 are shown in figures 18-21 below. CF_4 possesses the longest known lifetime of anthropogenic molecules (>50,000 yrs), which, when coupled with its high absolute radiative forcing (0.08 W m^{-2} ppb^{-1}, 6500 x eCO_2 (CO_2 equivalent, 100 yr time horizon)), can equate to upwards of 1% of total radiative forcing. Its primary emission source is as an unwanted by-product of aluminium smelting during a fault condition known as the Anode Effect. Thus the frequency of occurrence and duration of an Anode Effect event will determine the regional and global CF_4 emission. CF_4 has some additional minor applications in the semiconductor industry (as a source of F radicals), but industry has shied away from using CF_4 knowing that its GWP is so high. The aluminium industry has recognised the CF_4 (and C_2F_6) emission problem and has been undergoing processes of replacement of older, less efficient aluminium production cells with more efficient designs, and automated and quicker intervention policies to prevent the occurrence of these Anode Effects. It is also thought that CF_4 has a natural source from crustal degassing.

C_2F_6 is also a potent greenhouse gas with an atmospheric lifetime of >10,000 years. It has common sources to CF_4, this serves to help explain why all of the CF_4 above-baseline (pollution) events are usually correlated with those of C_2F_6. However, we note that there are many more frequent and greater magnitude emissions of C_2F_6 relative to CF_4. This is due to the dominant source of C_2F_6 being from semiconductor industries (plasma etching).

C_3F_8 (atmospheric lifetime 2600 years) is also used in semiconductor manufacturing, but to a lesser extent to that of C_2F_6. It also has an increasing contribution from refrigeration use. Observations of above-baseline C_3F_8 emissions are less frequent than those of C_2F_6 but are of a higher relative magnitude.

The current growth rates of atmospheric CF_4, C_2F_6 and the minor semi-conductor component C_3F_8 are 0.79, 0.08 and 0.02 ppt/yr respectively. These compounds tend to accumulate in the atmosphere due to their very long atmospheric lifetimes. In December 2012 the mixing ratio of CF_4 was 80.7 ppt, of C_2F_6 was 4.3 ppt and of C_3F_8 was 0.6 ppt.

SF_6 is an important greenhouse gas since it has a long atmospheric lifetime of 3,200 years, a high radiative efficiency and a considerable average atmospheric trend of 0.28 ppt/yr. It had reached a mixing ratio of 7.9 ppt by December 2012. Although having minor usage in the semiconductor industry, it is predominantly used in heavy duty electrical switchgear. Although the units themselves are hermetically sealed, breakdown and disposal, alongside leakage from wear-and-tear will cause this sector to emit SF_6. A minor use of this gas is also reported in its use as a blanketing (i.e. oxygen inhibiting inert gas) agent during magnesium production. Hence SF_6 will have many and more diffuse sources relative to the other perfluorinated species. Its atmospheric trend has been predicted to rise at a rate faster than linear, as older electrical switchgear is replaced by higher efficiency units.

5.3.2.1 PFC-14 (CF_4)

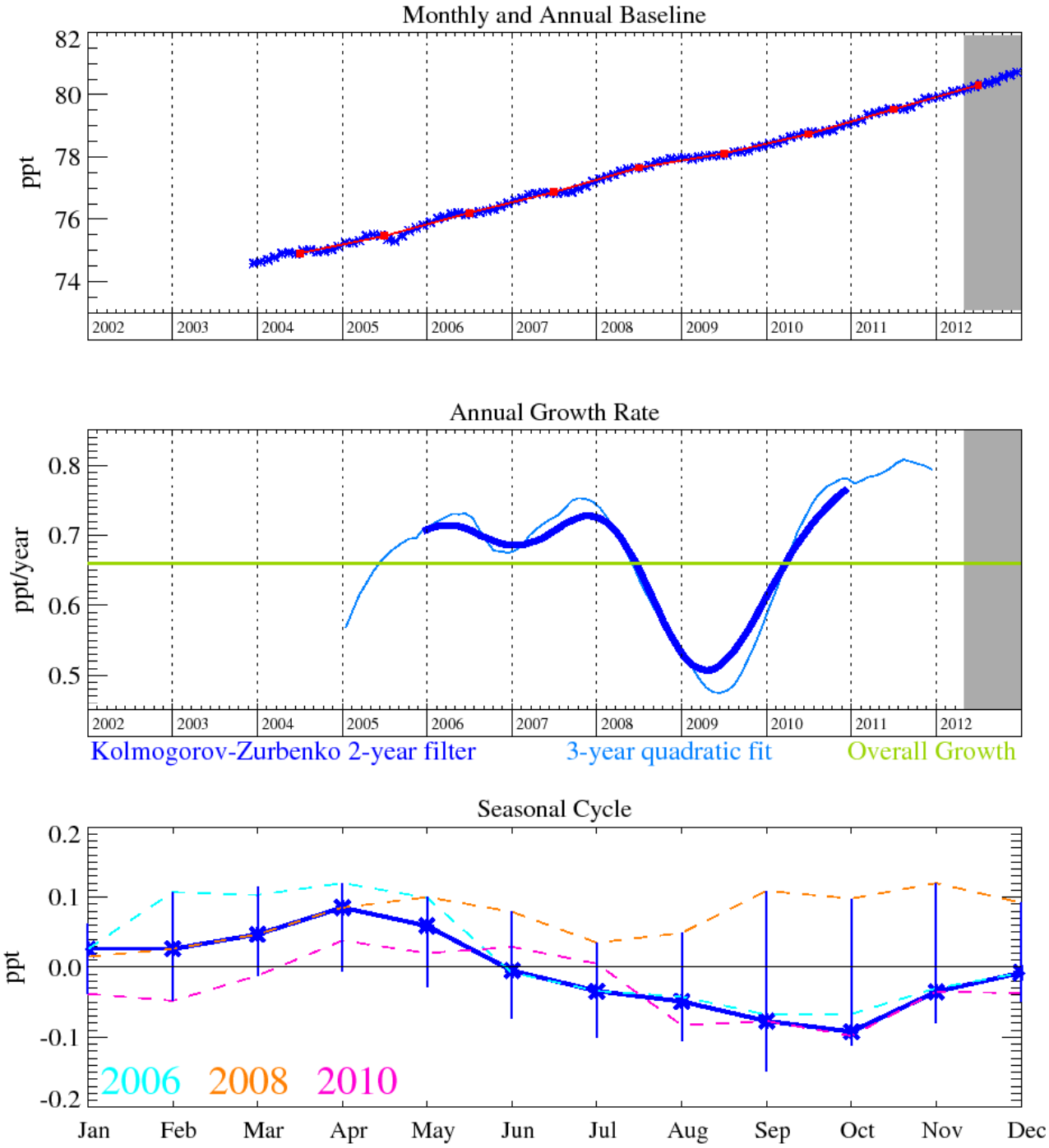

PFC-14 (carbon tetrafluoride, CF_4) is largely emitted as a by-product of aluminium production and, to a smaller degree, from the electronics industry. It has a GWP_{100} of 5,820, an RE of 0.10 W m^{-2} ppb^{-1} and a lifetime of over 50,000 years.

The grey area on each plot contains data that are unratified and therefore provisional.

Figure 18: PFC-14: Monthly (blue) and annual (red) baseline concentrations (top plot). Annual (blue) and overall average growth rate (green) (middle plot). Seasonal cycle (de-trended) with year to year variability (lower plot).

5.3.2.2 PFC-116

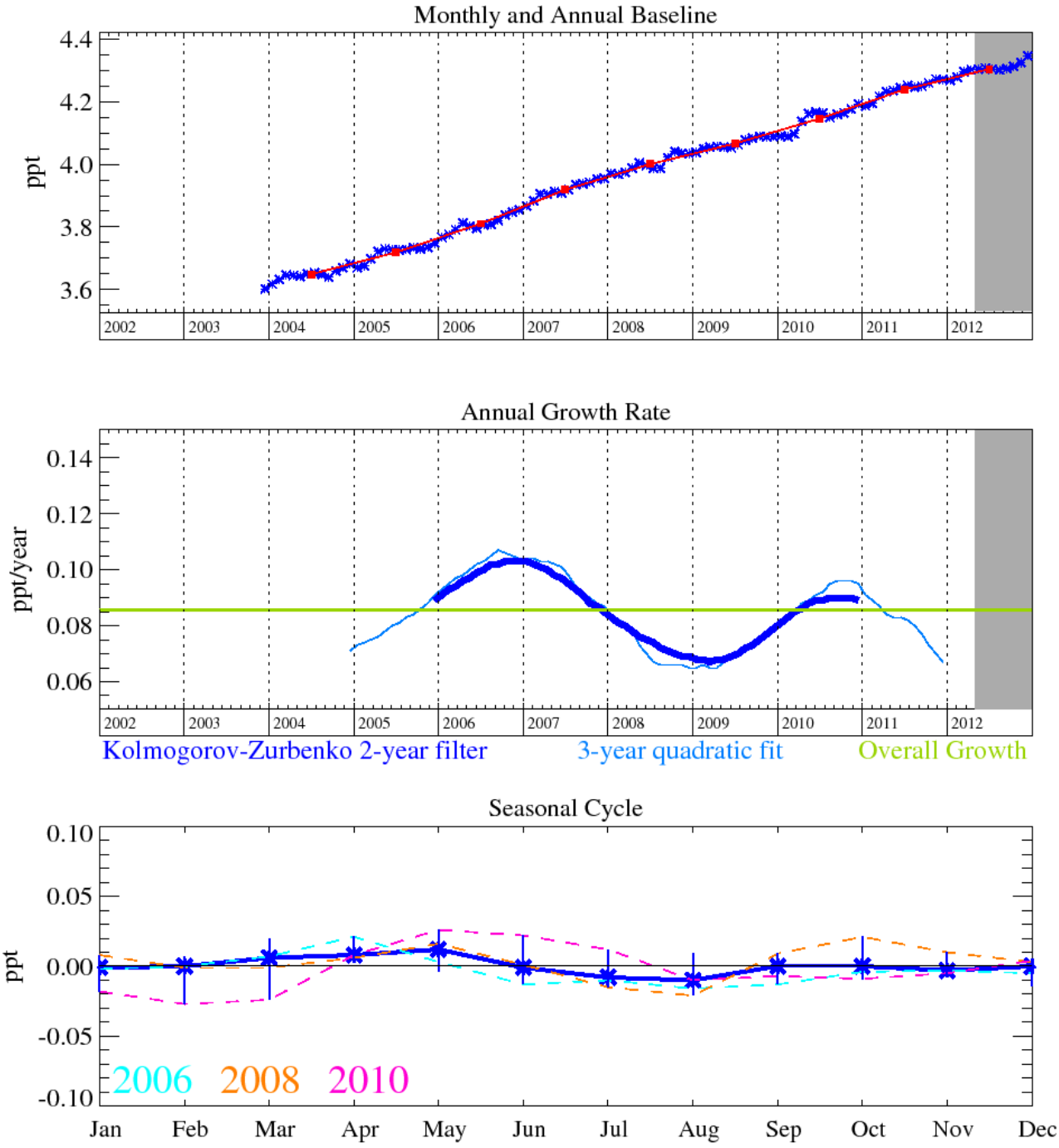

PFC-116 (perfluoroethane, CF_3CF_3) is emitted by the electronics industry and as a by-product of aluminium production. It has a GWP_{100} of 12,010, an RE of 0.26 W m^{-2} ppb^{-1} and a lifetime of over 10,000 years.

The grey area on each plot contains data that are unratified and therefore provisional.

Figure 19: PFC-116: Monthly (blue) and annual (red) baseline concentrations (top plot). Annual (blue) and overall average growth rate (green) (middle plot). Seasonal cycle (de-trended) with year to year variability (lower plot).

5.3.2.3 PFC-218

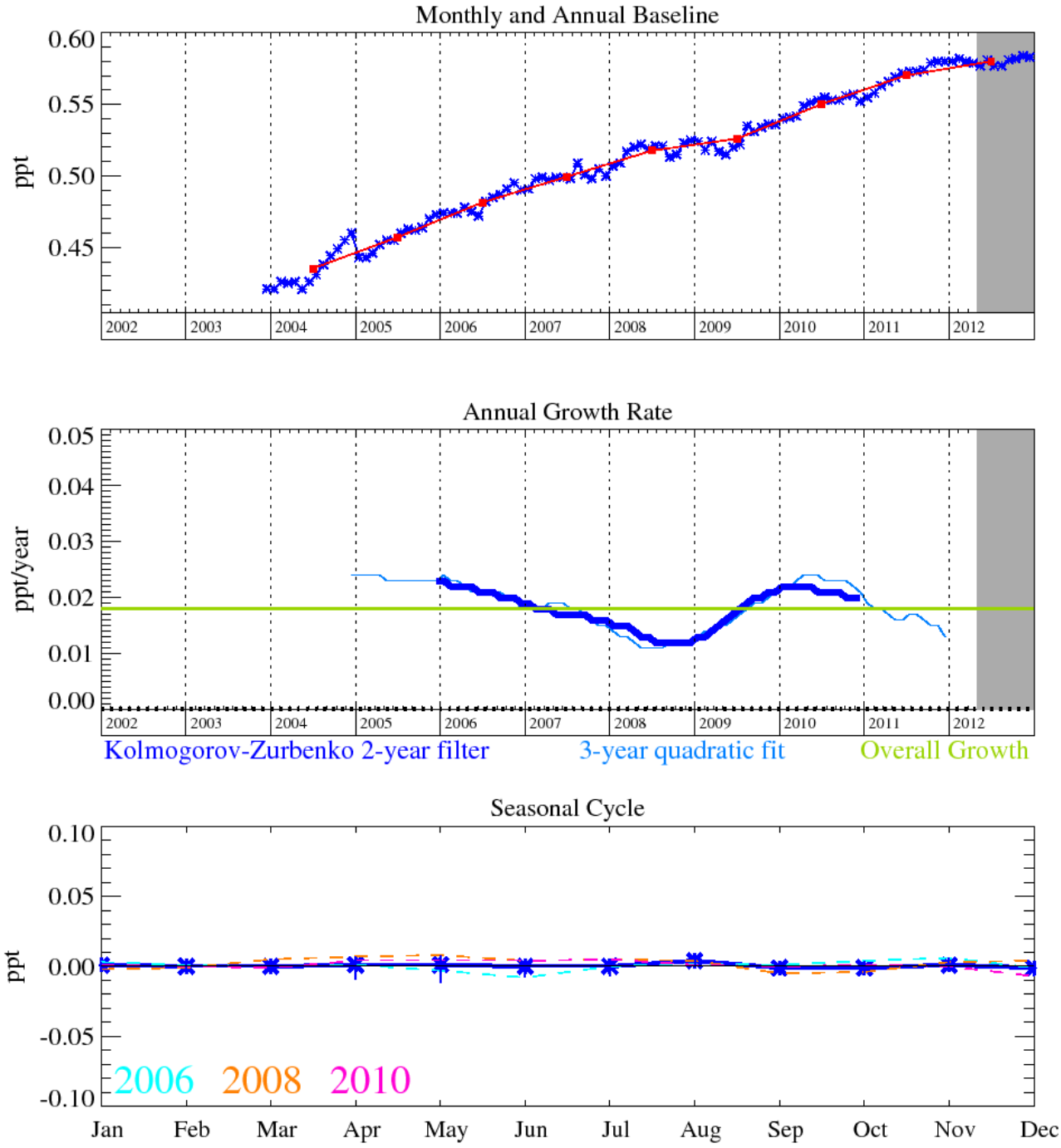

PFC-218 (perfluoropropane, $CF_3CF_2CF_3$) is largely emitted by the electronics industry, with very small contributions from aluminium smelting and increasing contributions from refrigeration use. It has a GWP_{100} of 8,690, a lifetime of 2,600 years and an RE of 0.26 W m^{-2} ppb^{-1}.

The grey area on each plot contains data that are unratified and therefore provisional.

Figure 20: PFC-218: Monthly (blue) and annual (red) baseline concentrations (top plot). Annual (blue) and overall average growth rate (green) (middle plot). Seasonal cycle (de-trended) with year to year variability (lower plot).

5.3.2.4 SF_6

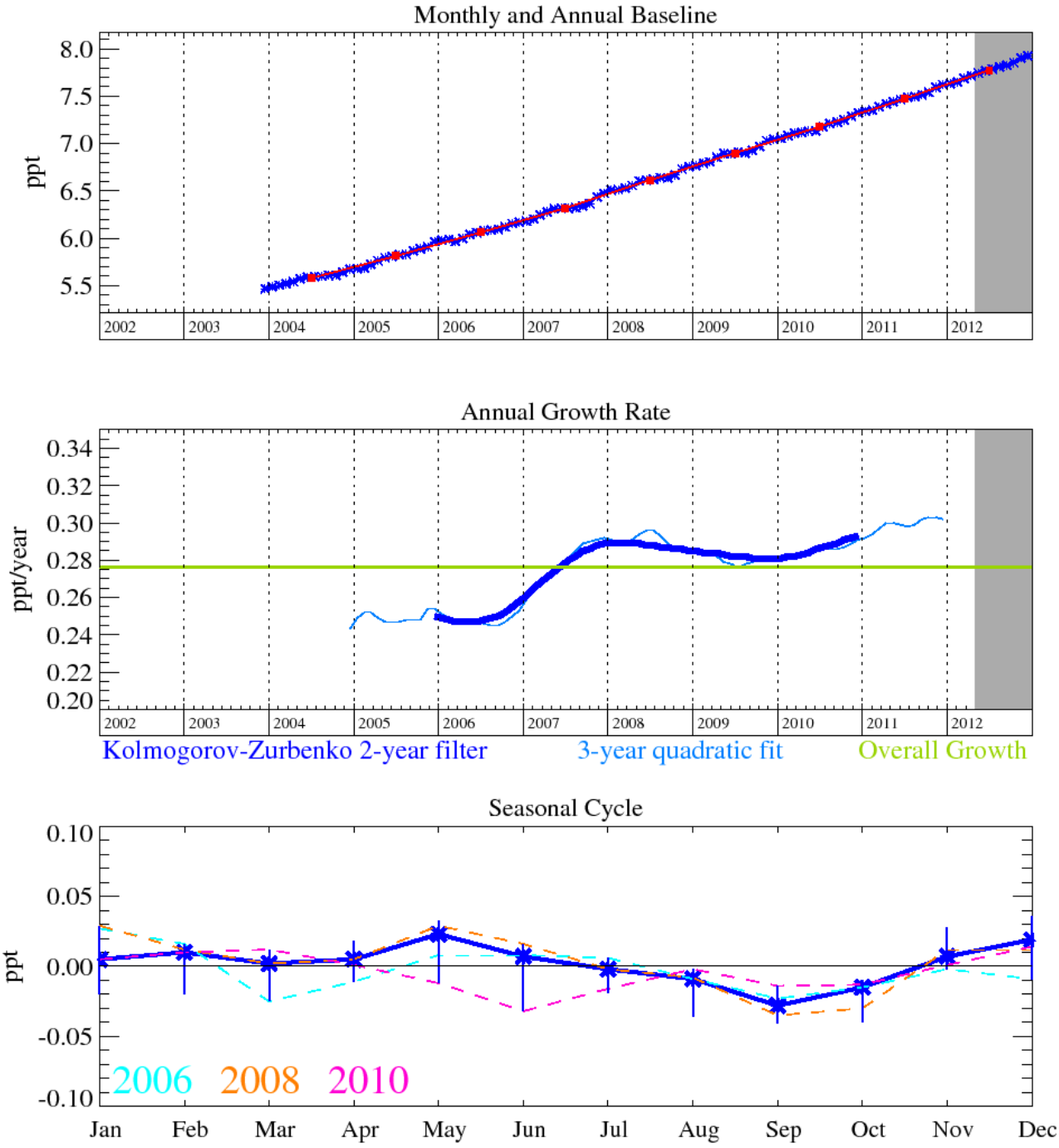

Sulphur hexafluoride (SF_6) is a very important greenhouse gas as it combines a high RE (0.52 W m^{-2} ppb^{-1}) with a very long lifetime (3,200 years). SF_6 concentrations are also expected to rise over the next several decades. Despite it having a huge GWP_{100} (22,800), it has a 0 ODP.

The grey area on each plot contains data that are unratified and therefore provisional.

Figure 21: SF_6: Monthly (blue) and annual (red) baseline concentrations (top plot). Annual (blue) and overall average growth rate (green) (middle plot). Seasonal cycle (de-trended) with year to year variability (lower plot).

5.3.3 Hydrocarbons

The long term trend for CH_4, shown in Figure 22, is of particular interest with a steep rise up to about 2000 followed by a flat period with almost no growth and then most recently a steep rise of up to 9 ppb/yr over the period 2007-2008, recent growth is estimated to be 5.3 ppb/yr with a mixing ratio of 1893 ppb in December 2012. The growth rate anomaly in 2007-2008 is unusual in that it occurred almost simultaneously at all of the AGAGE stations in both hemispheres.

In our annual report in 2009 we discussed how the mole fraction of CH_4 in the atmosphere had been rising considerably faster than its long term average growth rate. Several theories were postulated:

(1) Increased emissions from the high latitudes in the Northern hemisphere related to wetlands and reduced permafrost/snow cover.
(2) Increased emissions in the tropics due to increased emissions from wetlands/rice production or biomass burning due to El Niño conditions.
(3) Reduced levels of OH in the atmosphere. OH is the major sink for atmospheric CH_4.

However each of these theories in isolation does not seem to completely fit the evidence gathered so far. For example, there is no evidence for any link to large scale biomass burning (i.e. no concomitant increase in carbon monoxide), as was the case in 1998 driven by the largest ever El Nino drought. It was therefore our opinion that it is as yet too early to precisely pinpoint the cause for the elevated levels of CH_4 across the globe.

The inferences drawn from the observations were that the CH_4 increase is driven by wetland emissions in the boreal region (driven by a temperature anomaly) and in the tropics (possibly driven by a precipitation anomaly) with a small role for OH changes a possibility in the tropics but not statistically significant. The mole fraction of CH_4 reported from Mace Head (and other AGAGE stations) in 2009 indicate that the rise in CH_4 levelled out (as shown in Figure 22).

5.3.3.1 Methane (CH_4)

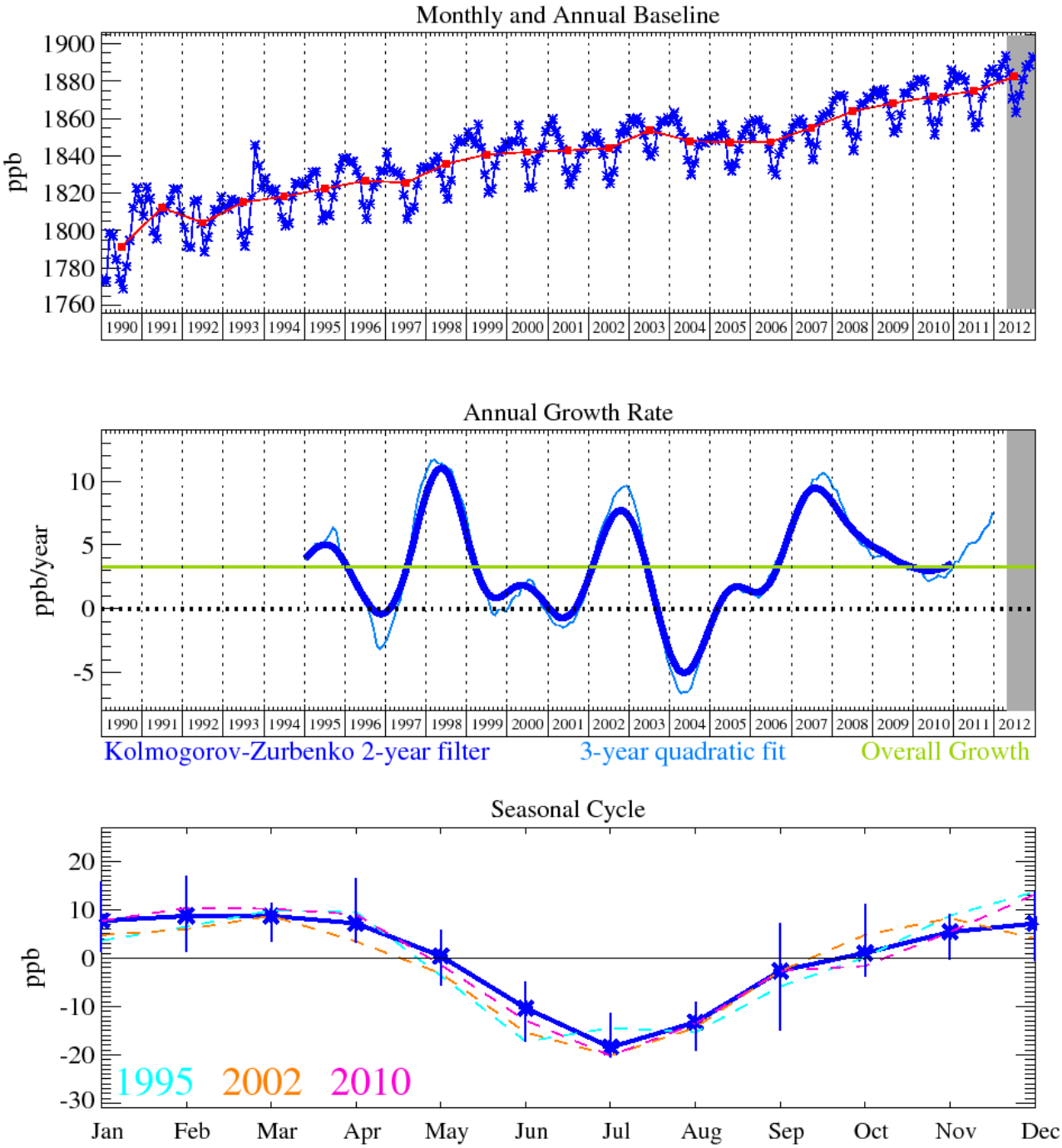

Methane (CH_4) is another naturally occurring compound and is the principal constituent of 'natural gas'. Wetlands, landfills and livestock comprise the main sources of CH_4. It does not destroy ozone and has an RE of 3.7×10^{-4} W m^{-2} ppb^{-1}. It has a modest lifetime of 12 years and has a GWP_{100} 25 times that of CO_2.

The grey area on each plot contains data that are unratified and therefore provisional.

Figure 22: Methane: Monthly (blue) and annual (red) baseline concentrations (top plot). Annual (blue) and overall average growth rate (green) (middle plot). Seasonal cycle (de-trended) with year to year variability (lower plot).

5.3.4 Carbon dioxide and nitrous oxide

CO_2 (Figure 23) is the most important greenhouse gas, and has steadily grown at an annual average rate of 1.9 ppm/yr, calculated from the baseline-selected monthly means. The most recent growth rate is estimated to be 2.1 ppm/yr. It has now reached a mixing ratio of 399 ppm (April 2012) which is the highest yet recorded at Mace Head, Ireland, and has shown significant growth rate anomalies in 1998/99 and 2002/03, which we suggest are a result of the global biomass burning events in those years.

Figure 24 shows the baseline monthly means and trend for N_2O with an almost linear upwards average trend of 0.72 ppb/yr. The most recent growth rate is estimated to be 0.97 ppb/yr. The mixing ratio in December 2012 was 325.8 ppb at Mace Head. The N_2O increase is attributable to human activities, such as fertilizer use and fossil fuel burning, although it is also emitted through natural processes occurring in soils and oceans. There are large uncertainties associated with the quantifying the sources of this gas. The global growth anomaly in N_2O is of particular interest with a very substantial increase in 2010-2011. At Mace Head the average historical growth rate of about 0.7 ppb/year has increased to over 0.8 ppb/year. Similarly in the Southern Hemisphere at Cape Grim, Tasmania the growth rate has increased from about 0.6 ppb/year in 2003 to about 1 ppb/year in 2011. From discussions with AGAGE colleagues these increases in N_2O emissions also may be linked to the tropics. Apparently 'wet and warm' microbes in soil can produce bursts in N_2O production, although this is less clear, as very saturated soils can decrease N_2O emissions, However, as noted by Dr R. Weiss of Scripps Institution of Oceanography, there may be different spatial distributions of "wetness" with increased N_2O emissions in some regions and decreases in others. Interestingly, hydrogen has also exhibited a growth spurt in 2011. Here wet soils tend to reduce the normal H_2 deposition velocities due to a reduction in diffusivity. At this stage more global sites need to be carefully assessed to confirm these increases in the N_2O growth rate. We expect AGAGE in collaboration with NOAA to address these issues in a forthcoming paper.

5.3.4.1 Carbon dioxide (CO_2)

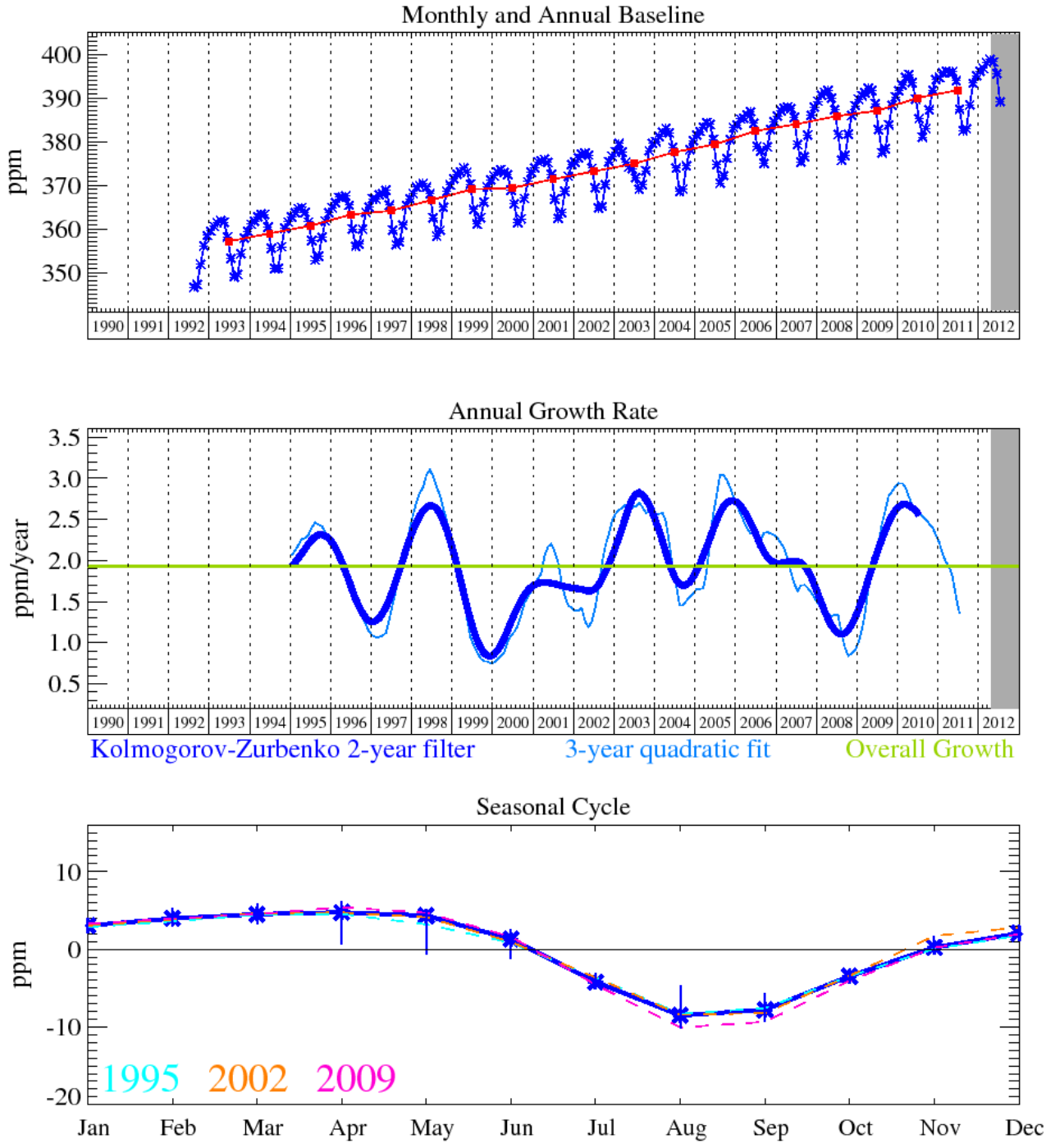

Carbon dioxide (CO_2) is perhaps the most famous of all greenhouse gases. It constitutes 0.039% of the atmosphere and is produced and destroyed continuously by an array of sources. It therefore has an indefinite lifetime and does not deplete ozone. As GWP is measured relative to CO_2, it is given a value of 1. Compared to thehalogen containing compounds it has a small RE (1.38×10^{-5} W m^{-2} ppb^{-1}).

The grey area on each plot contains data that are unratified and therefore provisional.

Figure 23: Carbon dioxide: Monthly (blue) and annual (red) baseline concentrations (top plot). Annual (blue) and overall average growth rate (green) (middle plot). Seasonal cycle (de-trended) with year to year variability (lower plot).

5.3.4.2 Nitrous oxide (N_2O)

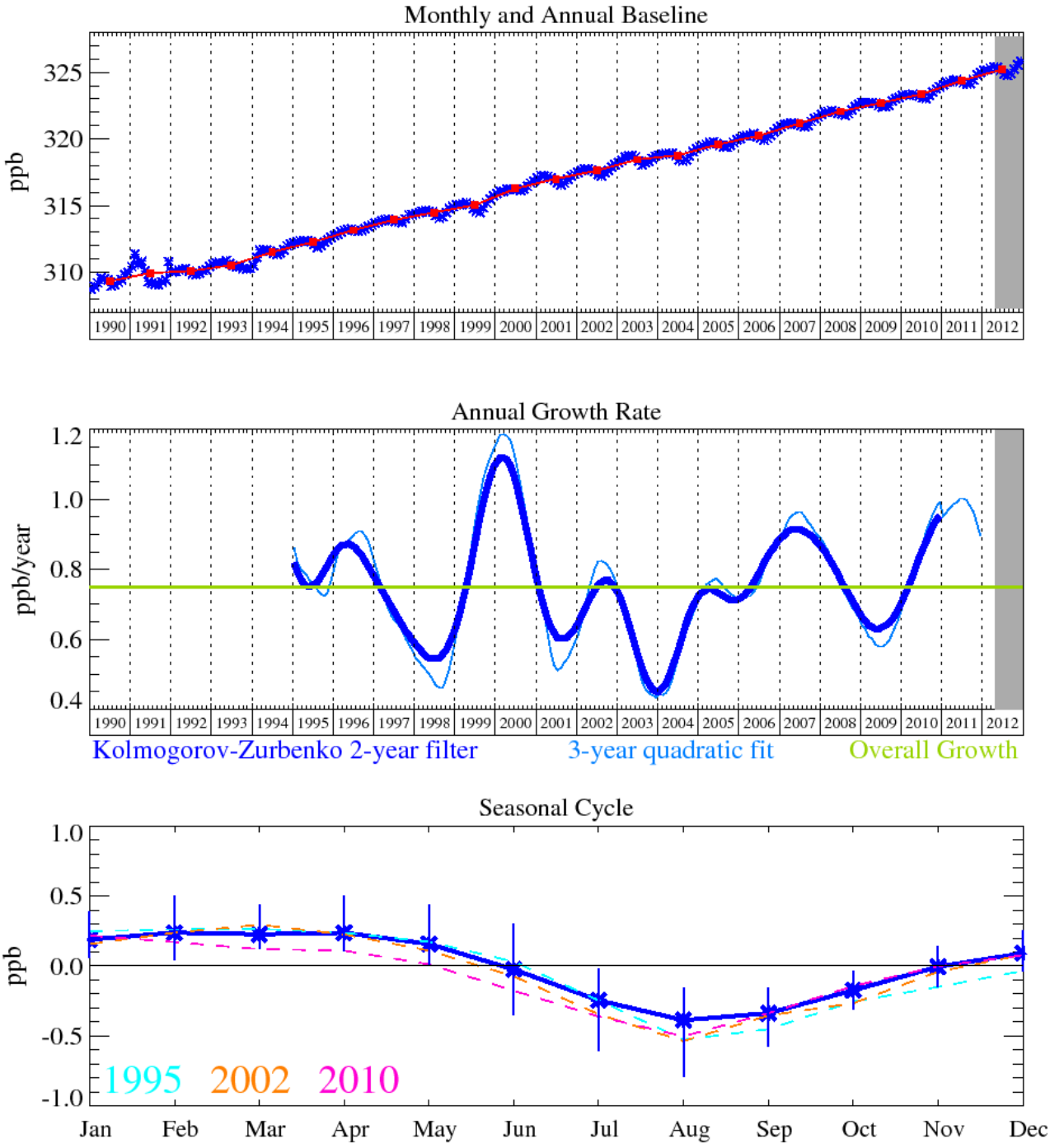

Although nitrous oxide (N_2O) does not destroy ozone directly, its photolysis leads to the ozone depleting compounds nitric oxide (NO) and nitrogen dioxide (NO_2). Recent studies have found N_2O emissions are currently the single most important emissions of a chemical that depletes ozone. It has a lifetime of 114 years, a GWP_{100} of 298, and an RE of 3.03×10^{-3} W m^{-2} ppb^{-1} N_2O is largely expected to increase with the development of biofuels and use of fertilizers.

Figure 24: Nitrous oxide: Monthly (blue) and annual (red) baseline concentrations (top). Annual (blue) and overall growth rate (green) (middle). Seasonal cycle (de-trended) with year to year variability (lower plot).